Technical Note

1967-41

Midlatitude F Region Densities and Temperatures at Sunspot Minimum

J. V. Evans

21 August 1967

Prepared under Electronic Systems Division Contract AF 19(628)-5167 by

Lincoln Laboratory
MASSACHUSETTS INSTITUTE OF TECHNOLOGY
Lexington, Massachusetts

The work reported in this document was performed at Lincoln Laboratory, a center for research operated by Massachusetts Institute of Technology, with the support of the U.S. Air Force under Contract AF 19(628)-5167.

MASSACHUSETTS INSTITUTE OF TECHNOLOGY
LINCOLN LABORATORY

MIDLATITUDE F REGION DENSITIES AND TEMPERATURES AT SUNSPOT MINIMUM

J. V. EVANS

Group 31

TECHNICAL NOTE 1967-41

21 AUGUST 1967

LEXINGTON MASSACHUSETTS

ABSTRACT

Results obtained for F region densities and temperatures using the Millstone Hill Ionospheric Radar for the year 1964 are presented. The measurements were made during 30-hour periods which followed at intervals of about two weeks throughout the year. The data obtained in each month have been averaged to yield a mean electron density profile and mean ion and electron temperature curves for each hour in the day. These curves were in turn used to construct plots showing contours of constant temperature and density as functions of altitude and time for each month. In addition, the annual variation of the midday and midnight densities and temperatures was obtained.

The seasonal anomaly in the F region peak electron density is evident though less pronounced than at years of high sunspot number. The F region layer thickness undergoes a smooth transition from winter to summer, being greatest in summer. It is shown that the daytime temperatures exhibit no marked seasonal dependence, and hence temperature effects (e.g., on reaction rates) cannot be invoked as the cause. The most striking nighttime phenomenon is the high electron temperature encountered in winter ($T_e/T_i \sim 2.0$) compared with summer. Evidence is presented for the existence of a flux of fast photoelectrons arriving from the conjugate ionosphere. The nighttime heating of the F region is thought to be caused by heat conducted down from the protonosphere together, in winter months, with the flux of fast photoelectrons from the conjugate hemisphere. During the daytime, heat appears to be conducted down through the 500-km altitude level at a rate of $\sim 5 \times 10^9$ eV/cm^2/sec. It is not clear whether the heat deposited in the protonosphere by fast photoelectrons is adequate to account for this energy, or if an additional source of daytime protonospheric heating is required.

Accepted for the Air Force
Franklin C. Hudson
Chief, Lincoln Laboratory Office

CONTENTS

MIDLATITUDE F REGION DENSITIES AND TEMPERATURES AT SUNSPOT MINIMUM

I. INTRODUCTION

Evans and Loewenthal,[1] in what subsequently shall be referred to as paper 1, have described the construction and operation of an ionospheric backscatter radar system at Millstone Hill that is used for obtaining F2 region electron densities, electron and ion temperatures on a routine basis. Evans[2] (in paper 2) has summarized the results obtained during the first year of operation (1 February 1963 – 31 January 1964). The present paper reviews the results obtained during 1964.

A number of changes in the manner in which the equipment is operated and the way in which the results are analyzed were made at the end of the first year. These are believed to have made a significant improvement to the accuracy of the results. These changes (described in Sec. II) removed small systematic errors that were present in the earlier results,[2] and lead us to place greater confidence in the absolute values of the temperatures presented here than those obtained in 1963.

Based upon the diurnal variation of temperature observed in 1963, Evans[3,4] has attempted to explain two anomalous features in the behavior of f_oF2 at Millstone Hill, namely, the summer and equinox evening increase and early morning (pre-dawn) winter increase. It is of interest, therefore, to see to what extent the 1964 results yield diurnal variations that are the same as those observed in 1963. For the most part, agreement between the two sets of results is remarkably good, and this lends considerable confidence to the results and to morphological descriptions given previously.[2-4]

New results are presented here which point to the existence of a large transport of heat from the protonosphere to the F region during the day. This result, together with the identification of F region temperature rises associated with the arrival of fast photoelectrons from the conjugate ionosphere, shed further light on the role of the protonosphere as a store of ionization and heat for replenishing the F region at night, and coupling the temperatures of the conjugate ionospheres together.

TABLE I

INCOHERENT BACKSCATTER OBSERVATIONS – 1964

Begin (EST)			End (EST)			Mean K_p
January 3	D	0900	January 4		1530	4_o
January 10	D	0900	January 11		1600	2+
January 17		1000	January 18		1600	2_o
January 31	D	1030	February 1		1600	3+
February 14		1030	February 15	q	1530	2_o
February 28		1500	February 29		1500	2+
March 13		0930	March 14		1600	2_o
March 27	q	0900	March 28	Q	1600	0+
April 10	q	0900	April 11		1600	2–
April 24	Q	0930	April 25		1600	2–
May 8	Q	0930	May 9	Q	1700	0+
May 22	q	1130	May 23		1500	1–
June 14		0800	June 15		1500	2–
June 27		0030	June 27		1500	1_o
July 10		0800	July 11		1500	2–
July 24	Q	1000	July 25		1530	1+
August 7		0830	August 8	q	1600	2–
August 21	q	1100	August 22		1530	2–
September 4		0800	September 5		1430	2_o
September 18	q	0800	September 19	Q	1530	1_o
October 2	q	0800	October 3		1500	1+
October 16	q	0800	October 17		1500	1+
October 30	Q	1100	October 30	Q	1630	1–
November 6	q	0900	November 7	Q	1600	1–
November 13	q	0900	November 14	Q	1500	0+
November 27	q	0900	November 27	q	1500	0+
December 3		0900	December 4	q	1600	1_o
December 17		0900	December 18		1530	2_o
December 29		0900	December 30		1600	1_o

II. OBSERVING PROCEDURE

In 1963, the complete height range over which density and temperature measurements could be made (about 200 to 800 km) was examined once every 90 minutes, approximately. Observations were usually conducted for periods of 30 hours at a time at weekly intervals. During 1964, the interval between observing periods was increased to two weeks, but the time required to obtain complete density and temperature profiles was reduced to one hour. Thus, the number of profiles obtained was only about 25 percent less than in 1963. This reduction in the amount of time to produce the profiles was accomplished by recording some of the signals for later non-real-time processing. Table I lists the periods during which the data were gathered, and indicates the mean value of the geomagnetic index K_p during these periods. It can be seen that, apart from January, the days on which the equipment was operated were magnetically quiet.

Several changes were made to the equipment in order to increase its reliability and ease of operation, but these did not appreciably alter the sensitivity of the apparatus.[1]

III. DATA REDUCTION

Prior to 1964, the electron and ion temperatures obtained from the radar signal spectra at Millstone Hill tended to overestimate T_i. The error (of the order of 10 percent) arose from the neglect in the computation of expected spectrum shapes (paper 1) of the distortion introduced in the receiver by gating from the timebase a portion equal in length to the transmitted pulse. That is, the frequency smearing introduced by transmitting a pulse was allowed for, but the additional broadening arising from gating the receiver was not. Thus, an entirely new set of theoretical spectra $P(f)_{obs}$ have been computed using the proper weight function which allows for these instrumental effects (F. Perkins, H. Tagfors, private communication).

$$P(f)_{obs} = \int_{-\infty}^{+\infty} \langle |S(f)|^2 \rangle_{avg} F_i(f)\, df \quad , \tag{1}$$

where $\langle |S(f)|^2 \rangle_{avg}$ is the power spectrum at the output of the receiver and $F_i(f)$ is the power spectrum response of the analyzer filters (assumed to be equal). The power spectrum $\langle |S(f)|^2 \rangle_{avg}$ presented to the spectrum analyzer filter bank is

$$\langle |S(f)|^2 \rangle_{avg} = \int_{-\infty}^{+\infty} d\nu \, \langle |H(\nu t_o)|^2 \rangle_{avg} \cdot \frac{4\tau}{[2\pi(f-\nu)]^2} \cdot \left[1 - \frac{\sin 2\pi(f-\nu)\,\tau}{2\pi(f-\nu)\,\tau}\right] , \qquad (2)$$

where $\langle |H(\nu t_o)|^2 \rangle_{avg}$ is the spectral broadening (of a CW signal) introduced by the ionosphere (as a function of frequency ν) corresponding to a delay t_o, and τ is the pulse length employed. The equations for $\langle |H(\nu t_o)|^2 \rangle_{avg}$ have been given by a number of authors, e.g., Fejer.[5]

Besides being a function of electron to ion temperature ratio T_e/T_i, ion temperature T_i and ion composition, the spectrum shape depends upon the electron density N. Evans and Loewenthal[1] showed that this latter dependence could be handled by obtaining from the experimental results an approximate electron density profile from which the density N could be estimated. The values of T_e/T_i and T_i were then established by comparison of the observed signal spectra with ones computed for the same density. In practice, only a limited number of cases for different densities were worked out, namely, corresponding to plasma frequencies f_N = 1.0, 1.5, 2.0, 2.5, 5.0, and 10 Mcps ($N = 1.24 \times 10^4 f_N^2$, N in electrons/cm^3, f_N in Mcps). For the wavelength in use at Millstone Hill (λ = 68 cm), it transpires that the signal spectrum shape ceases to change when $f_N \geq 5$ Mcps.

In the new computations, theoretical spectra have been computed only for the case f_N = 10 Mcps. Following the suggestion of Moorcroft,[6] these are employed to derive values of T_e/T_i and T_i which will be correct if $f_N \geq 5$ Mcps. If the plasma frequency is less than ~5 Mcps, only T_i will be correct, and the derived electron-to-ion temperature ratio $(T_e/T_i)'$ will be related to the true ratio (T_e/T_i) in

$$\left(\frac{T_e}{T_i}\right)' = \frac{\alpha^2}{1+\alpha^2}\left(\frac{T_e}{T_i}\right) \quad , \tag{3}$$

where $\alpha = \lambda/4\pi D$ and $D = \sqrt{kT_e/4\pi Ne^2}$ is the Debye length. For Millstone, $\alpha = 0.785\sqrt{N/T_e}$ when the density N is expressed in el/cm^3. It follows that it is a relatively simple matter to produce a set of curves from which T_e can be read off, given N and T'_e.

The procedure for analyzing the data is now as follows. The signal spectra are scaled to yield two quantities: f, the width in kcps between the center and a value of half peak intensity, and x, the ratio of the peak intensity (in the wings) to that at the center frequency. These values are inserted on a graph appropriate to the pulse length employed (τ = 0.5 or 1.0 msec) to yield values of T_i and T'_e/T_i. The electron density profile is then obtained in the manner outlined previously[1] except that the factor employed to correct for the effect of the temperature inequality ($T_e > T_i$) becomes[6]

$$N(\text{true}) = \frac{2}{1 + T'_e/T_i}\, N(\text{obs}) \quad , \tag{4}$$

which is a closer approximation than used hitherto,[1,2] namely,

$$N(\text{true}) = \frac{2}{1 + T_e/T_i}\, N(\text{obs}) \quad . \tag{5}$$

Given the true density N at the height where the temperature measurement was made, the true value of T_e is obtained by interpolation from a plot of T_e vs T'_e and N [Eq. (3)] as outlined above. As in the past, the method by which the electron density profiles are constructed depends upon the radar data only for the height and shape of the profile. The absolute density at all heights is established by normalizing the peak density to the value of $N_{max}F2$ observed with an ionosonde.

From all these data, mean hourly electron density and temperature profiles are constructed for each month. In the case of the density N, this requires that the relative density N/N_{max} must be determined at fixed intervals, e.g., ±25, ±50, ±75, ±100 .... km with respect to the peak. A mean of these

is obtained yielding a mean profile with the correct shape. This is then assigned the mean value of h_{max} and N_{max}. For the temperature profiles, the mean electron and ion temperatures at the heights sampled are computed and the best smooth curve drawn through these points. These vertical profiles are then used to plot contours of constant density N (expressed as a plasma frequency f_N) and temperature as a function of height and time over the day. This type of presentation provides the greatest amount of reduction in the number of data points obtained.

In addition to the analysis outlined above, mean daytime and nighttime temperature profiles for each month are constructed by averaging all the data obtained during the periods 0900-1500 EST and 2100-0300 EST, respectively. These curves are then used to obtain plots of isothermal contours vs height and month for the entire year. These plots may be employed to infer daytime and nighttime seasonal variations.

IV. ACCURACY OF THE RESULTS

It is thought that sources of instrumental error,[1] which were bothersome during the first half of 1963, had all been eliminated by 1964.[2] Accordingly, the principal sources of systematic error are the assumptions made during the analysis. The first of these is that only 0^+ ions are present at all heights. There is some evidence[7] that at the lowest altitude observed, i.e., with the pulse center at 225 km, regions with an appreciable percentage of NO^+ or O_2^+ ions are included by the large vertical extent of the pulse (±35 km approximately). The amount of this error introduced in the temperature results appears to be −10 percent or less, and is significant chiefly in lowering the value of T_i obtained at this altitude by about 50°K.

At the highest altitudes (> 600 km) there is the possibility that a small number of light ions are present. This would lead to an overestimate of T_i and somewhat smaller overestimate of T_e'. The exact height of the transition region from 0^+ ions to H_e^+ and H^+ ions is known to be lowest at sunspot minimum.[8,9] There is also evidence that it is higher during the day than at night and that it is higher at temperate latitudes than over the equator.[10] Unfortunately, no satellite-borne mass-spectrometer measurements for 1964 have been

published. Yet by various indirect methods the height of the transition altitude has been inferred for this period. Watt[11] has employed topside soundings obtained with the Alouette I sounder together with certain assumptions concerning the behavior of the electron and ion temperatures with altitude to infer the transition height. At the dip latitude of Millstone (73°), Watt[11] finds that the transition altitude (defined as the height of 50% 0^+, 50% H_e^+ or H^+ ions) lies above the satellite (i.e., > 1000 km) during the day and at ≥ 900 km during the night. The altitude of the transition lies sufficiently beneath the satellite that it can be located with reasonable certainty only over the range of dip latitudes 48° to 60°. Using the same satellite, Barrington, et al.[12] were able to infer some information concerning the ion composition at 1000 km altitude by determining the cutoff frequency of a VLF emission together with the scale height of the F region at the satellite. At a height of 1000 km above Millstone (L = 3.5), Barrington, et al.[12] find less than 20% H^+ ions during 6-hour periods centered on 0600 and 1800 local mean time. The only recent rocket flights into the topside ionosphere from which ion composition could be determined indicated that H_e^+ never became the predominant ion.[9] Bauer has suggested that this is typical behavior at sunspot minimum,[9] in which case the estimates of Barrington, et al., concerning the H^+ abundance may be taken as close to the total abundance of light ions.

From the foregoing, it would appear that the upper limit at which temperature determinations can be made with this apparatus (approximately 800 km by day and 600 km by night) lies at least one scale height (i.e., ~200 km) below the transition altitude at all times. We may expect, therefore, that the light ion abundance is of the order of 10 percent or less at the highest altitude that can be examined. Thus, we believe that the error introduced by the neglect of the presence of light ions is substantially less than postulated earlier (paper 1).

V. DIURNAL VARIATIONS

A. Electron Temperature

The variation of the electron temperature T_e, ion temperature T_i, and an electron density plasma frequency f_N for an equinoctial, summer, and winter

month are shown in Figs. 1a-c to 3a-c, respectively. During equinoctial months (March, April, September, and October), the electron temperature (Fig. 1a) rises rapidly at sunrise, is roughly constant at all altitudes throughout the day, and falls somewhat less rapidly at sunset. During the day, there is a positive temperature gradient of about 2°/km above 300 km and ~ +6°/km below. At night, the gradient is about 1.5°/km at all altitudes. Similar electron temperature behavior is observed in summer (Fig. 2a), although there appears to be an early morning maximum at some altitudes. In winter (Fig. 3a), the temperature gradient above 300 km is higher than in summer (~3°/km), but the actual temperature near $h_{max}F2$ is lower. At night in all seasons, the electron temperature exceeds the ion temperature. This is thought to be a consequence of heat supplied by the protonosphere[13] as argued previously;[2] however, it is probable that during the winter months when the conjugate hemisphere remains sunlit, photoelectrons traverse the protonosphere and contribute to the nocturnal heating of the local ionosphere (Secs. VII, VIII-B).

During the short summer night, the electron temperature is roughly constant at a given altitude. In the equinoxes, the temperature reaches a minimum a little before midnight (Fig. 1a) and then increases again. In winter, the same thing happens except that the reversal from cooling to warming occurs only 2 hours after local sunset. This behavior is believed to be a consequence of the fact that the protonospheric heat flux is roughly constant throughout the night[14] and the heat loss (from electrons to ions) initially exceeds the input, but later as the density decreases this situation is reversed.

B. Ion Temperature

The diurnal variation of T_i above 300 km altitude tends to follow that of the electron temperature, thereby demonstrating the thermal coupling between the two. During the daytime, the ion temperature remains fairly constant at all altitudes. In summer, T_i declines throughout the night. In winter, T_i shows little evidence of sunset and does not decrease appreciably till 0200 EST when the electron temperature is also found to be declining rapidly. In Ref. 3, we argued that this was a consequence of the increase in density (Fig. 3c) which

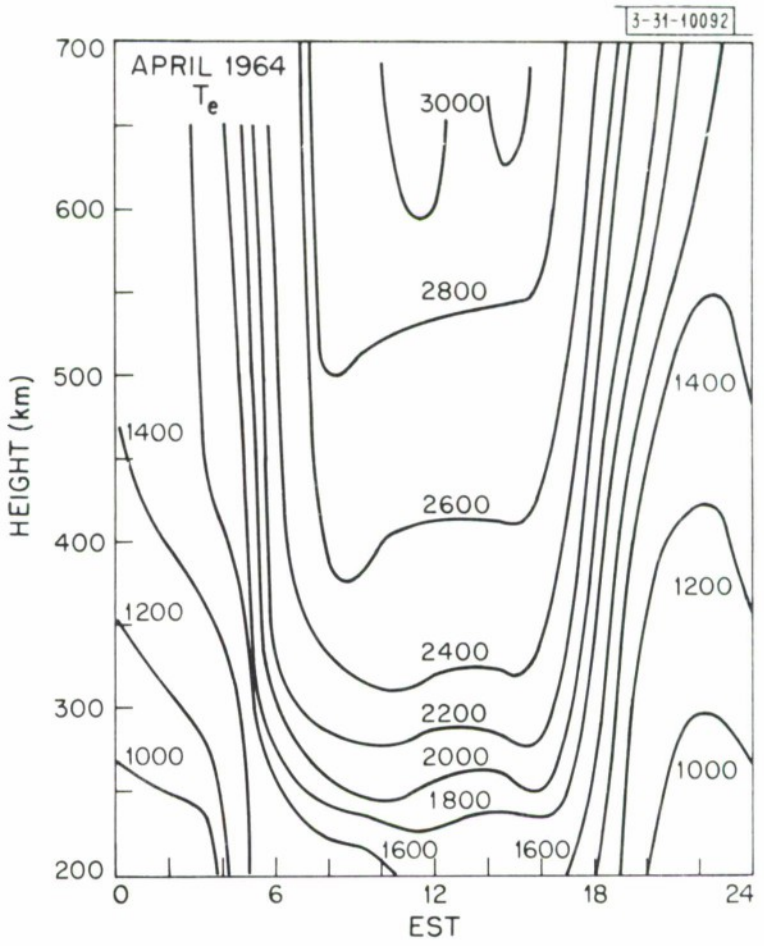

Fig. 1a. Equinox behavior: diurnal variation of electron temperature.

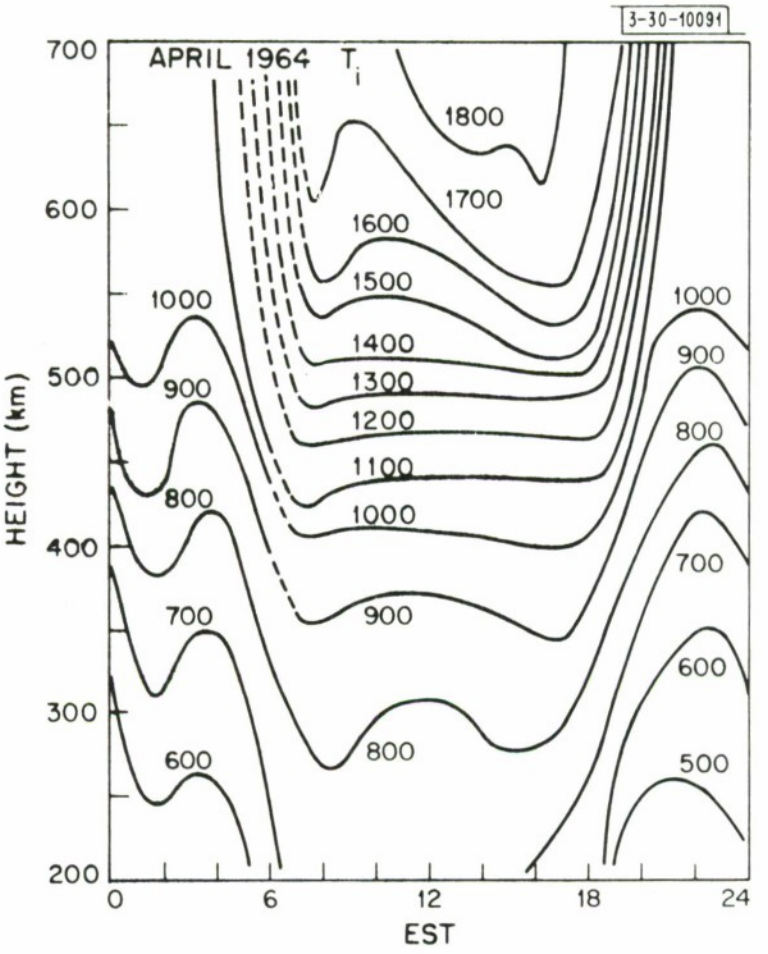

Fig. 1b. Equinox behavior: diurnal variation of ion temperature.

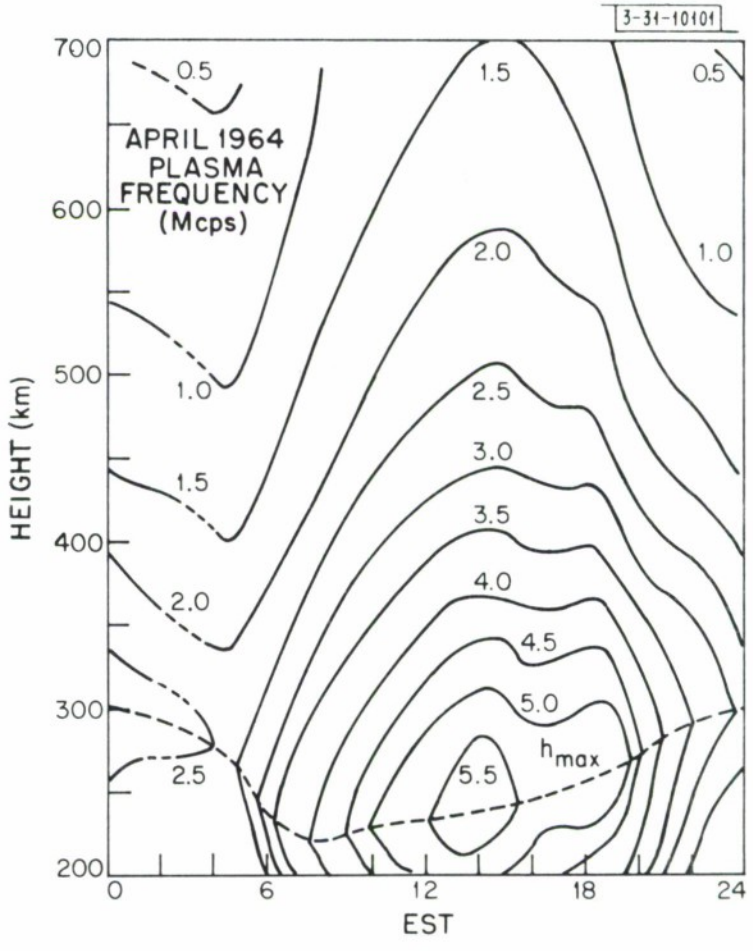

Fig. 1c. Equinox behavior: diurnal variation of plasma frequency f_N.

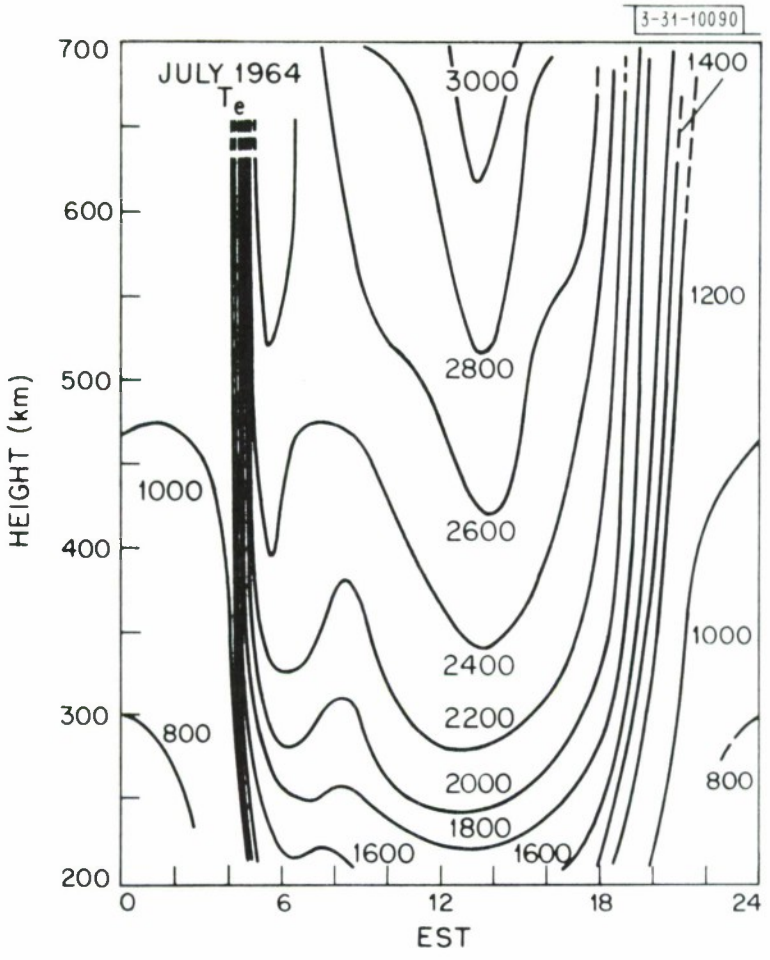

Fig. 2a. Summer behavior: diurnal variation of electron temperature.

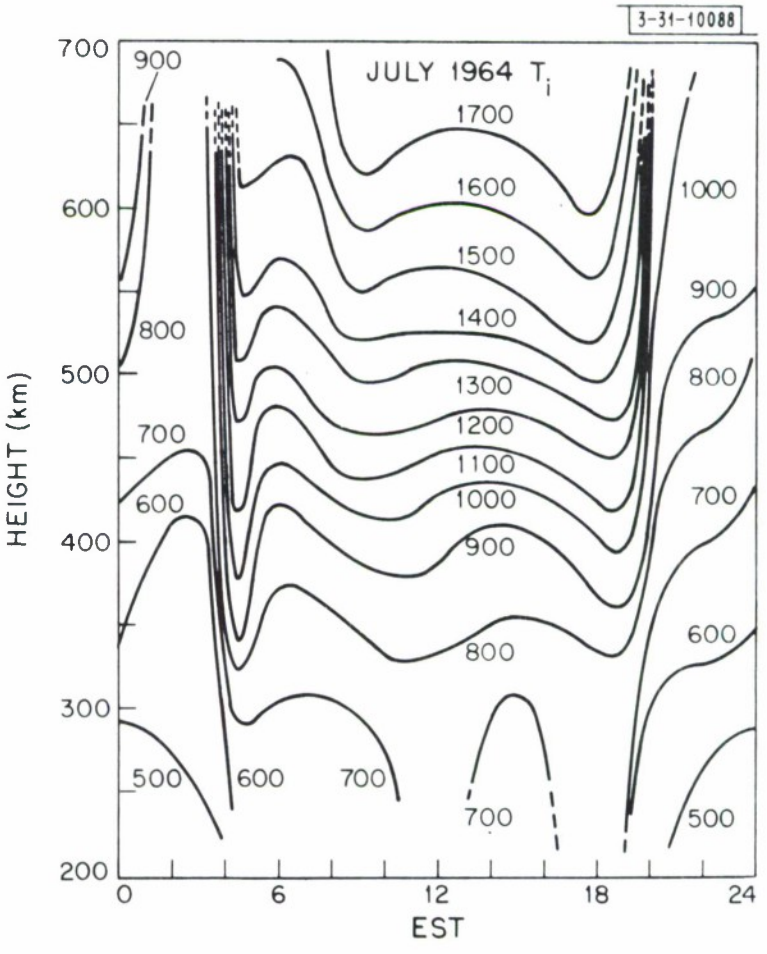

Fig. 2b. Summer behavior: diurnal variation of ion temperature.

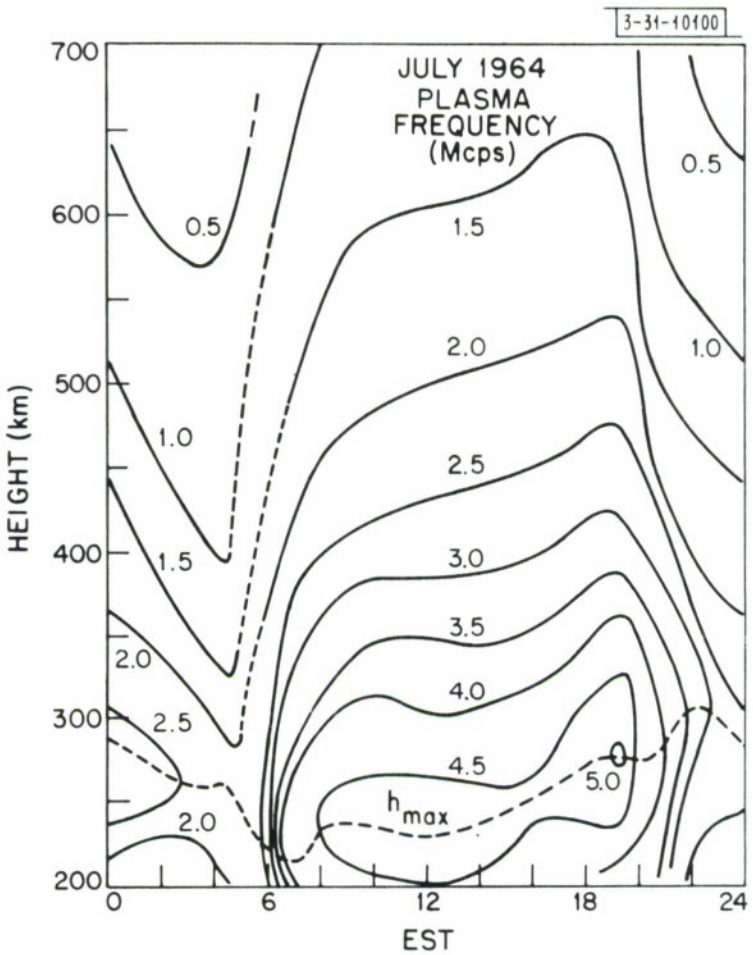

Fig. 2c. Summer behavior: diurnal variation of plasma frequency f_N.

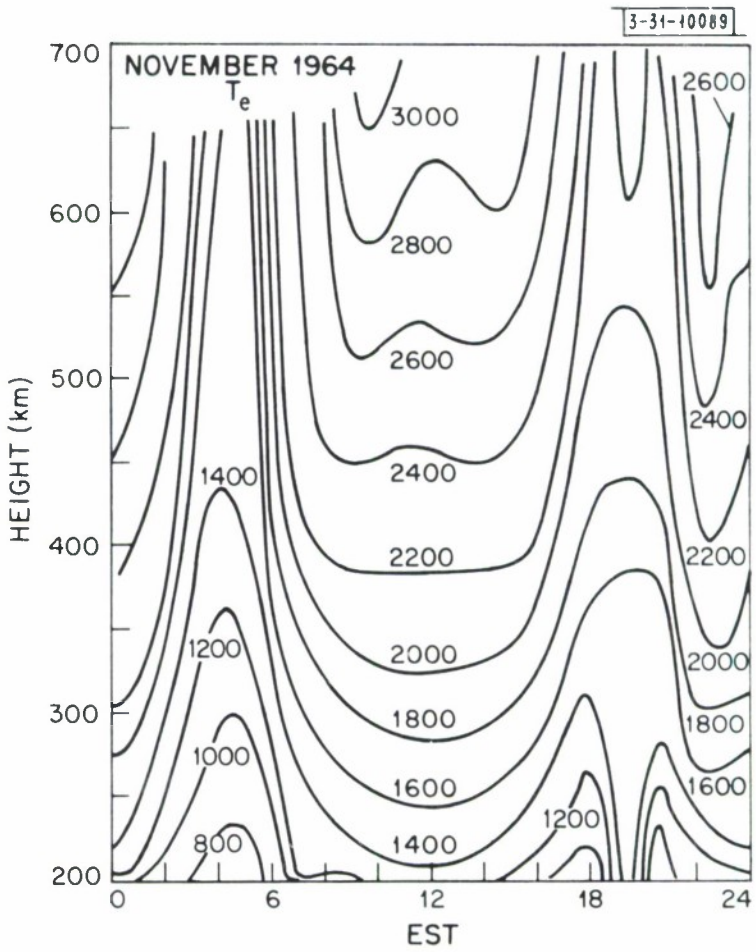

Fig. 3a. Winter behavior: diurnal variation of electron temperature.

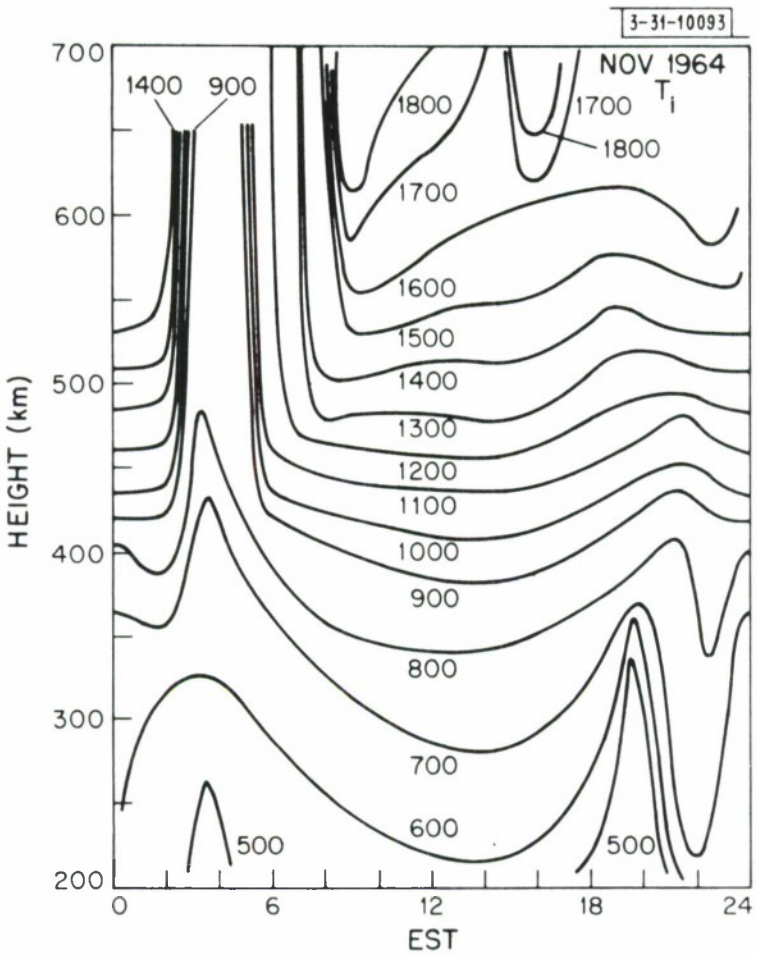

Fig. 3b. Winter behavior: diurnal variation of ion temperature.

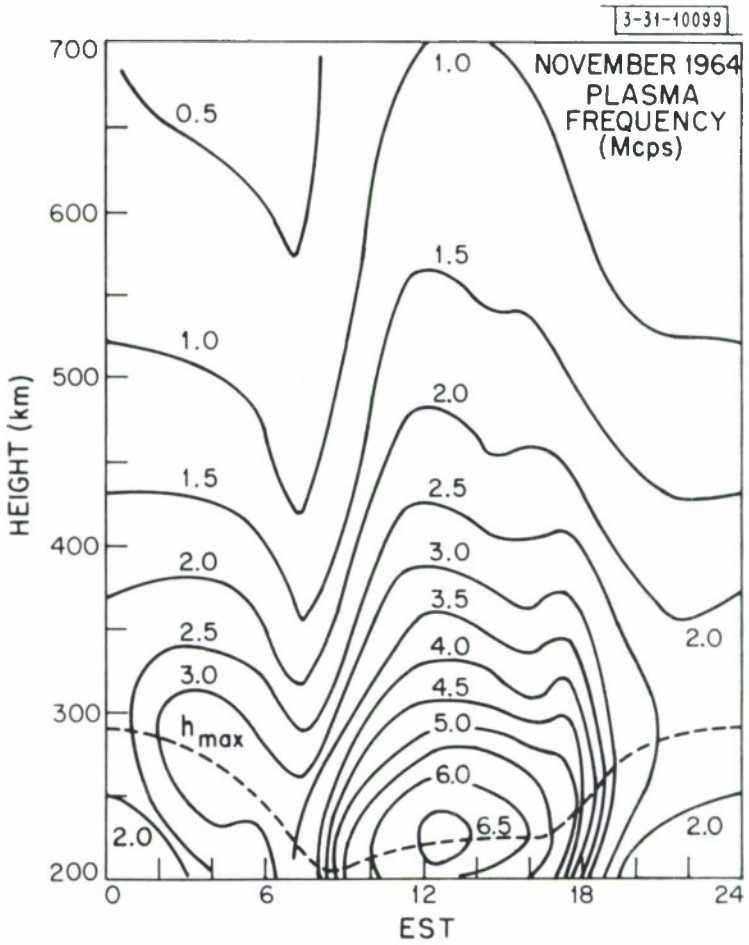

Fig. 3c. Winter behavior: diurnal variation of plasma frequency f_N.

occurs at this time and causes a second reversal in the balance between heating and cooling. These new results serve to support this conclusion.

In all seasons, the daytime temperature gradient above 400 km is of the order of 4°/km, suggesting that the ion temperature is greater than that of the neutrals, and is converging on the electron temperature. Below 300 km, the ions are probably in good thermal equilibrium with the neutrals, but the values shown in Figs. 1b and 3b (toward the bottom of the figures) are probably too low (Sec. IV). During the night in equinox and in summer, the temperature gradient dT_i/dh appears somewhat lower than during the day (~1.5°/km).

C. Electron Density

The behavior of the electron density (Figs. 1c and 3c) shows a striking degree of similarity from month to month. For example, h_{max} is always highest (~290 to 300 km) near midnight and falling between midnight and dawn. The value of h_{max} reaches a minimum about 2 hours after ground sunrise (Table II) and thereafter tends to rise, with the rate of increase being fastest after sunset.

The electron density increases throughout the morning at all altitudes and tends to reach a maximum around noon or shortly thereafter. If one allows for the fact that the layer is rising, then it is clear that at fixed heights with respect to h_{max} the density tends to decrease in the afternoon at all altitudes until the evening increase occurs. This phenomenon has been the subject of a separate paper[3] where it was suggested that the rapid fall of electron temperature during sunset gives rise to a collapse in the layer thickness and an increase in the density at the peak. In summer, this is sufficiently pronounced for f_oF2 to reach its highest value at this time of day. Variability in the increase of f_oF2 from day to day is probably related to the height to which h_{max} has risen during the course of the day. Thus, although the rapid fall in electron temperature seems to be the prime physical agent, the forces that are responsible for driving the layer upward may exert a modifying influence. The evening increase is evident in all months at heights well above h_{max} but can be recognized in f_oF2 only during equinox and summer. Evans[3] suggested that this is because (1) in winter, the fall in T_e is neither large nor rapid,

TABLE II

GROUND SUNRISE AND SUNSET AT MILLSTONE HILL AND ITS MAGNETICALLY CONJUGATE POINT

	Millstone Hill (42.60°N 71.5°W)		Conjugate Point (71.91°S 80.7°W)		
Date	Sunrise EST	Sunset EST	Sunrise EST		Sunset EST
April 1	5.30	1810	7.10		1745
April 15	5.10	1830	8.15		1630
May 1	4.45	1845	9.40		1500
July 1	4.15	1935	↕	Always dark	↕
July 15	4.25	1920			
August 1	4.40	1910	11.25		1335
November 1	6.20	1645	2.21		2140
November 15	6.40	1630	↕	Always sunlit	↕
December 1	7.55	1620			

(2) in winter, the amount of ionization above h_{max} that can participate is less, and (3) the density at the peak is already high.

In summer, the evening maximum in f_oF2 is larger than the noon maximum, but in equinox the midday maximum tends to be the larger. In winter, as already noted, the evening increase is an observable effect only above about 300 km altitude, so that f_oF2 shows a single midday maximum. In summer and equinox the densities decrease at all altitudes throughout the night. In winter, this decrease is arrested near 2200 EST at heights below 450 km and a maximum occurs near 0400. Above 500 km, the density appears to be decreasing throughout the night. It has been suggested[4] that this redistribution of ionization in the F region is caused by the cooling of the whole protonosphere. Whatever the cause, the total ionization present at 0400 is higher than that at 2200 EST. The only possible source of such ionization is the protonosphere. Local production (by any possible ionizing agency) is ruled out because the electron density would then be increased, whereas in fact it is found to be decreasing at this time. We discuss this phenomenon further in Sec. IX.

VI. SEASONAL VARIATIONS

A. Electron Temperature

Figures 4a and b show the variation of the mean daytime (0900-1500) and mean nighttime (2100-0200) electron temperatures. The daytime results (Fig. 4a) show no pronounced seasonal variation below 300 km altitude. Above 300 km, there appear to be real variations, for example, a summer minimum and equinoctial maxima, as noted in 1963.[2] At night, there is a very pronounced seasonal trend. The temperatures are lowest in summer (June and July) and increase uniformly into the winter. As noted in Sec. V, this is thought in part to be a consequence of a higher protonospheric heat flux due to the fact that the conjugate ionosphere then remains sunlit in winter. Also, fast photoelectrons arriving from the conjugate ionosphere serve to heat the local ionosphere in winter but not in summer (Secs. VII, VIII-B).

B. Ion Temperature

The comments made above for electron temperature can partly be applied to the ion temperature shown in Figs. 5a and b. The daytime averages show no seasonal trend, but at night the temperatures are clearly highest in winter and lowest in summer. The summer to winter difference in T_i at night is considerably less than for T_e, indicating that the latter is a far better indicator of nocturnal heating. No good explanation can be offered for why the nighttime temperature is so low in August (Fig. 5b). The magnetic activity on the days of observation in this month (Table I) was not particularly different from that encountered in any other month.

C. Electron to Ion Temperature Ratio

Figures 6a and b show the variations of T_e/T_i over the year. As may be expected from the foregoing, the daytime values (Fig. 6b) show no pronounced seasonal variation, while at night the lowest values are encountered in summer and the highest in winter. The peak daytime value (Fig. 6a) is somewhat higher than the peak value reported previously.[2] This is because the computed spectrum profiles employed for comparison in 1963 were inaccurate (Sec. III). The

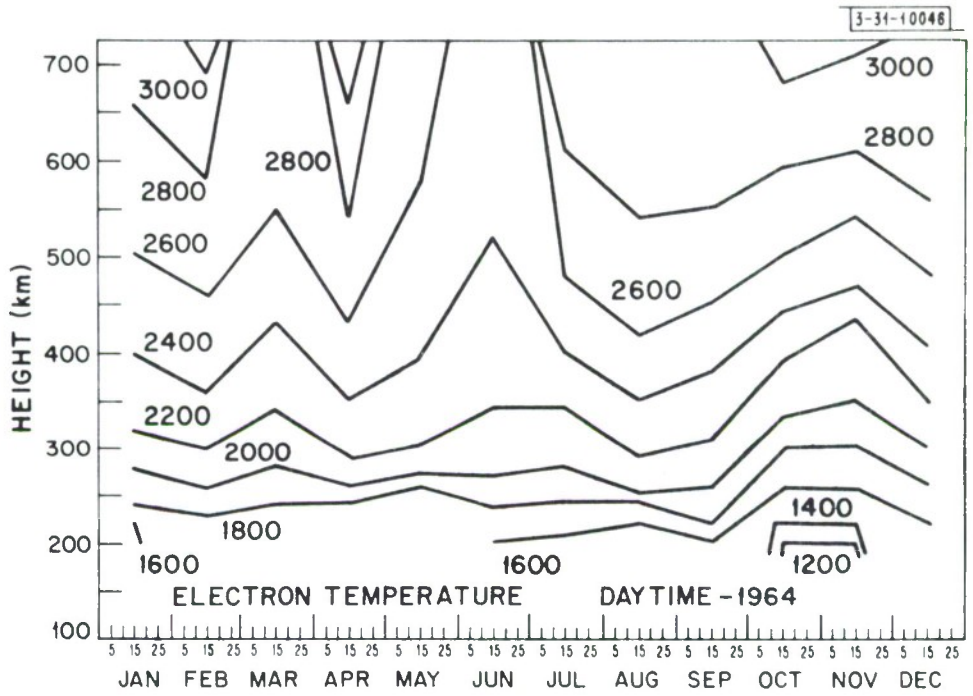

a. Mean daytime (0900-1500 EST).

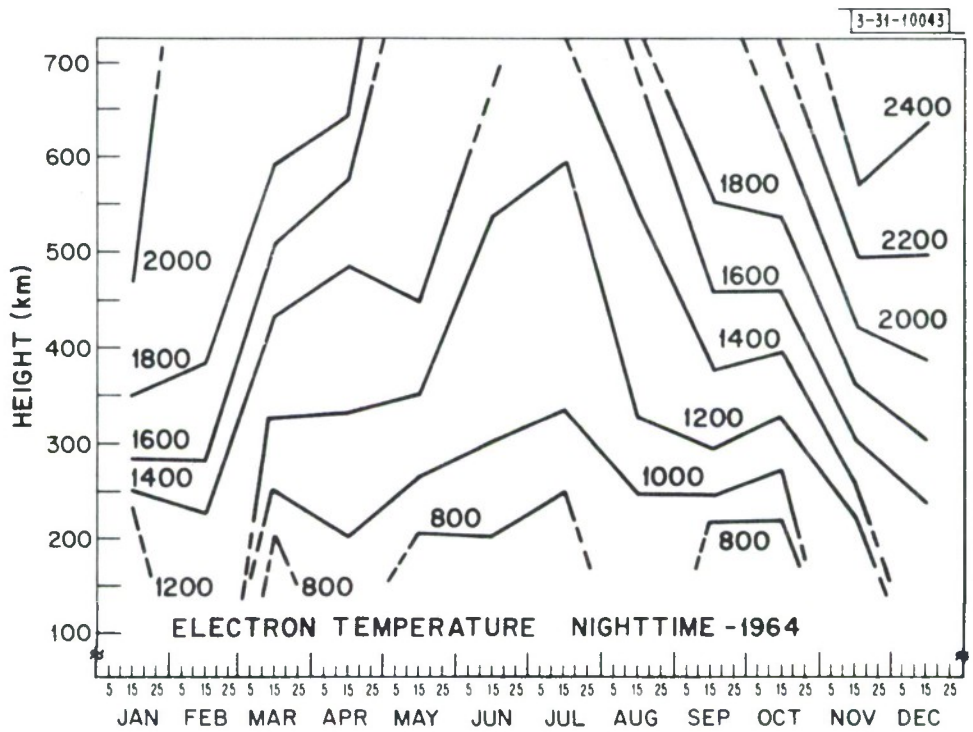

b. Mean nighttime (2100-0300 EST).

Fig. 4. Seasonal variation of electron temperature.

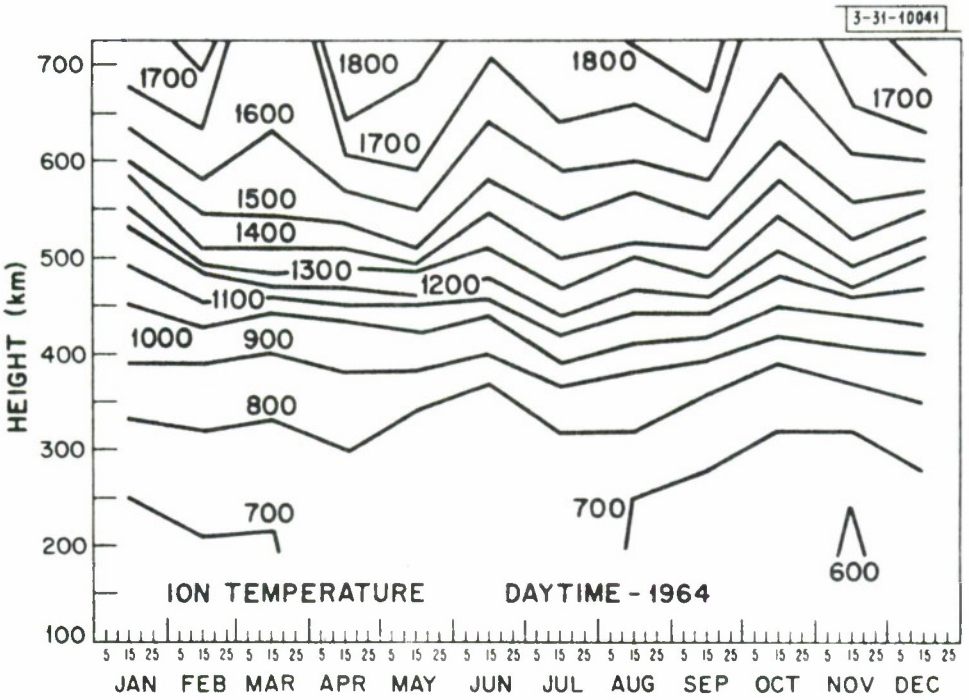

a. Mean daytime (0900-1500 EST).

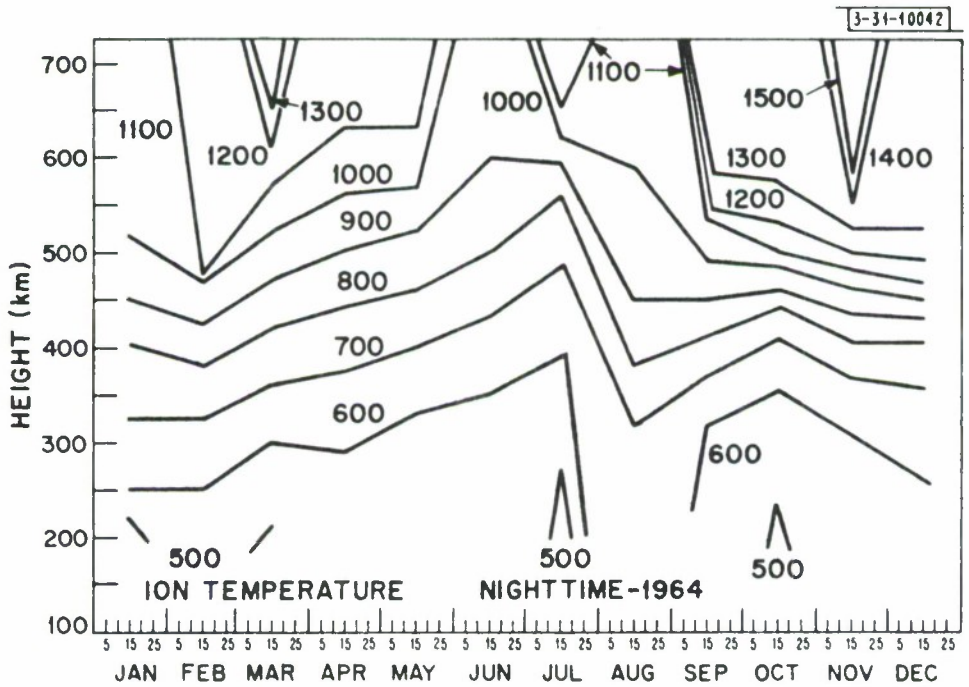

b. Mean nighttime (2100-0300 EST).

Fig. 5. Seasonal variation of ion temperature.

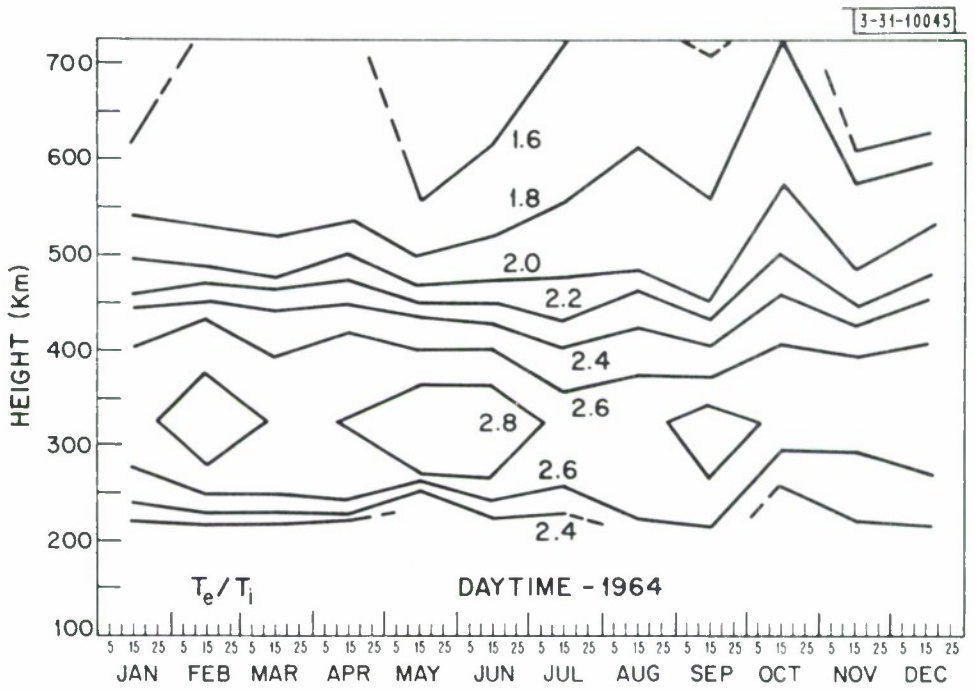

a. Mean daytime (0900-1500 EST).

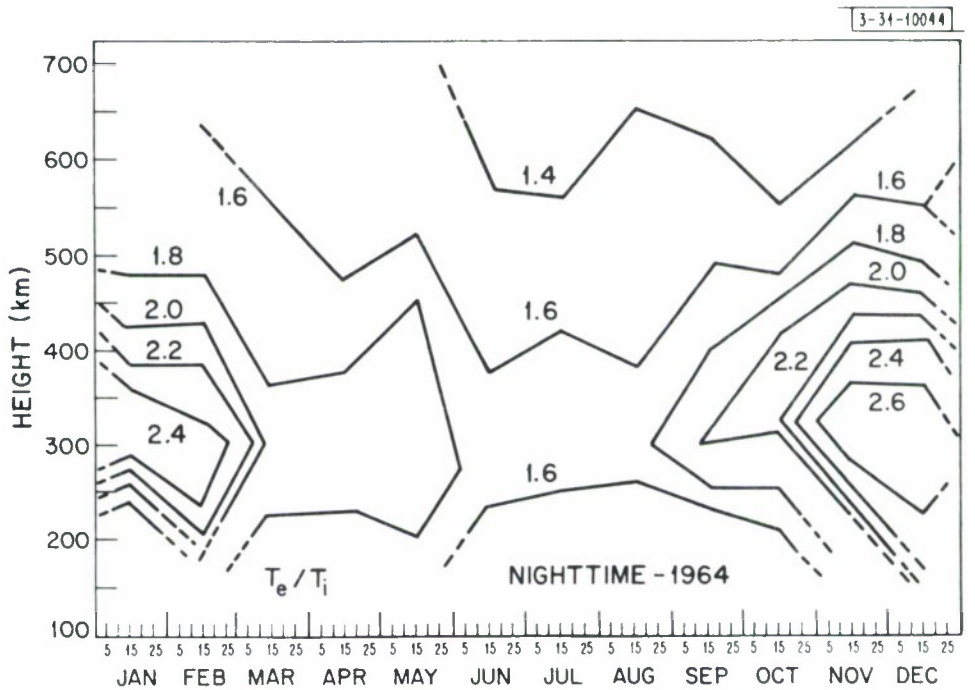

b. Mean nighttime (2100-0300 EST).

Fig. 6. Seasonal variation of T_e/T_i.

peak always lies between 300 and 350 km, irrespective of season, and has a value in the range 2.6 to 3.0. At 600 km altitude, T_e/T_i has declined to about 1.6. At night, the peak is found to lie at about the same altitude, but has a value which varies markedly with season, being ~2.6 to 2.7 in winter and 1.6 to 1.7 in summer. However, at 600 km the variation is less – from about 1.4 in summer to about 1.6 in winter.

D. Electron Density

It would not be meaningful to take 6-hour averages of the electron density. We have, however, plotted the noon contours of constant plasma frequency in Fig. 7. The lowest critical frequency values were encountered in August and the highest in November and December. When comparing Figs. 4a, 5a, and 6a with Fig. 7, we find that there does seem to be some correspondence between density and temperature during the period July to December. The electron temperature at the peak of the layer decreases by ~200°K from summer to winter and at 300 km the decrease is ~300°K. The ion temperature decreases

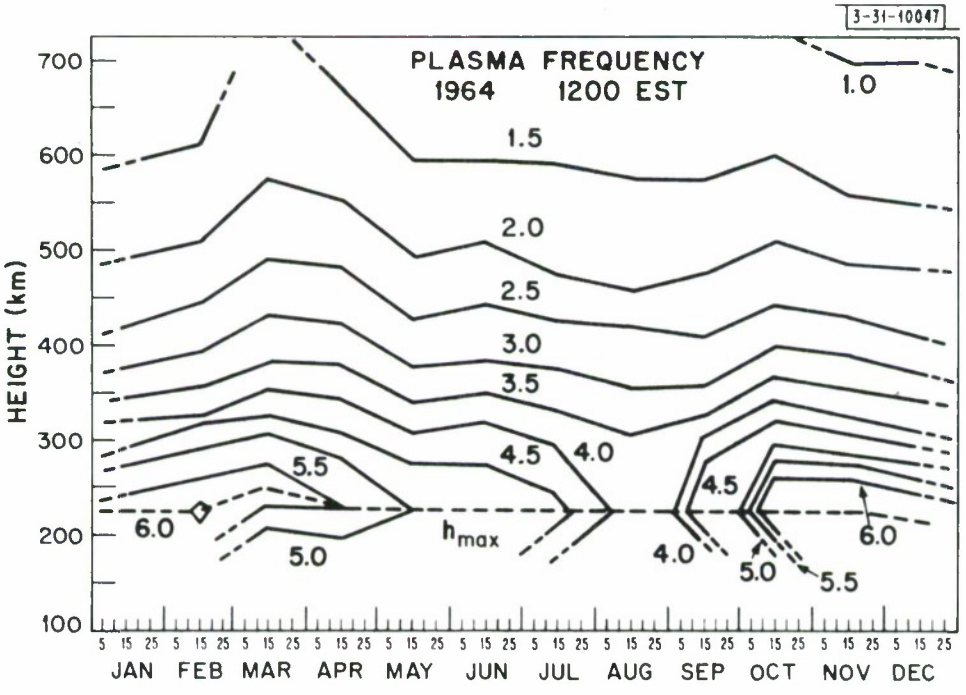

Fig. 7. Seasonal variation of plasma frequency at midday.

by about 100°K in this height interval. These variations do not seem to be supported by the results for the first part of the year. The only parameter that definitely shows a variation correlated with f_oF2 is T_e/T_i at h_{max}. However, the variation is small – from 2.4 in summer to 2.6 in winter.

Figure 7 illustrates several features of the seasonal anomaly. It is striking that the anomaly is strictly a feature of the peak of the layer. At an altitude of about 400 km or above, highest densities tend to occur in the equinoxes, and it is evident from Fig. 7 that the total content $\int_{200}^{700} Ndh$ is a maximum at these times. This is confirmed by Faraday rotation measurements.[15] Thus, the high values of f_oF2 in winter arise as a result of greater densities near the peak of the layer that are not reflected in the profiles substantially above h_{max}. That is, the scale height immediately above the layer is smaller in winter than at any other time. This is shown most clearly in Fig. 8 where we have

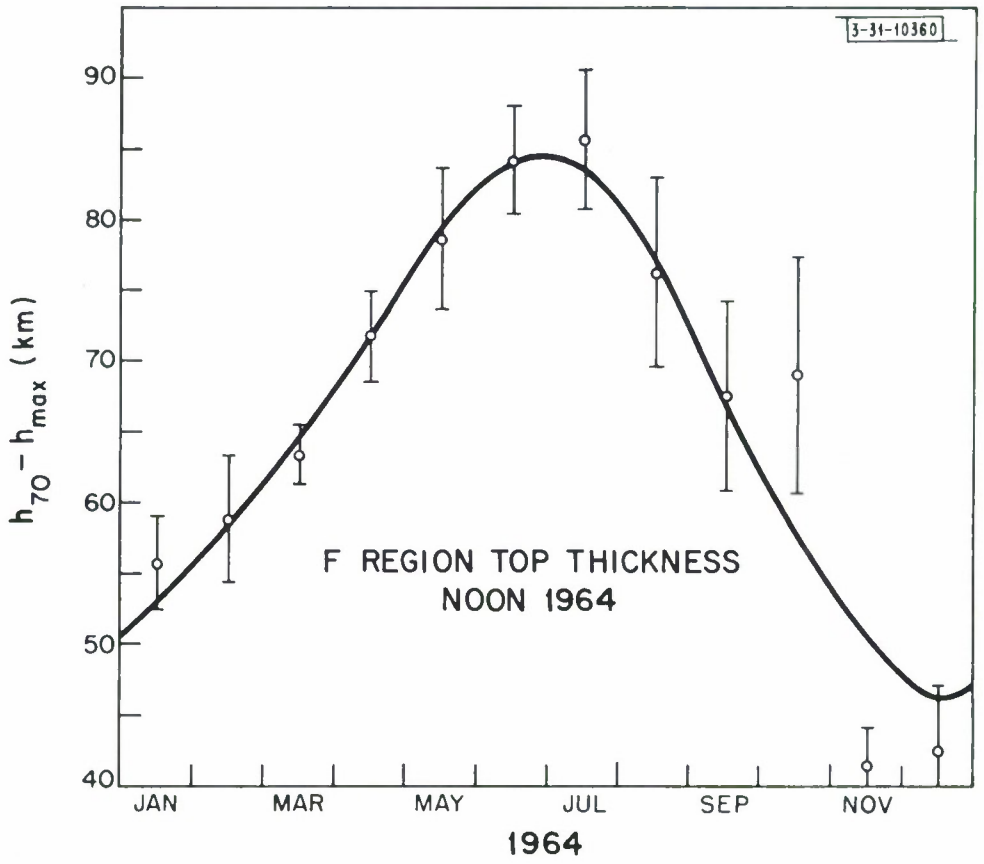

Fig. 8. Seasonal variation of the thickness of the upper part of the F region, h(70% – h(max).

plotted the height interval required for the density to fall from N_{max} to a value 0.7 N_{max} above the peak. Figure 8 shows the mean monthly variation of this thickness parameter at noon in 1964. The two profiles nearest noon on each of the days listed in Table I were used to compute the mean and the error bars are probable errors derived from the scatter of the values. It can be seen that there is only an annual variation in this parameter, the minimum being in winter.

The parabolic semi-thickness of the lower part of the layer also varies smoothly from a summer maximum to a winter minimum.[16] This striking change in layer shape has also been demonstrated by the seasonal variation in the "slab thickness" parameter [= $(\int Ndh)/N_{max}$] determined from Faraday rotation measurements.[15] It is clear from the foregoing that the slab thickness apparently does not vary throughout the year as a consequence of large changes in T_e and T_i as suggested by Yeh and Flaherty.[15] Thomas[17] has discussed the changes in layer shape that might result from changes in T_e, T_i or T_e/T_i. For the most part these are small, but in any event the absence of major daytime seasonal variations in these quantities (Figs. 4a, b – 6a, b) shows that an explanation for this seasonal variation of layer thickness (by almost a factor of two) must be sought elsewhere. The neutral temperature T_n is a maximum in the solstices and a minimum in summer and winter,[18] and hence variations in T_n cannot be invoked as an explanation either. Thus, it appears impossible to invoke temperature changes which result in either changes of the height distribution of the constituents or the reaction rates of the loss processes[19] to explain the seasonal anomaly.

VII. PHOTOELECTRONS FROM THE CONJUGATE IONOSPHERE

In paper 2, we drew attention to a pre-dawn increase in electron temperature occurring in March. Since that time, Carlson[20-22] has shown that the phenomenon is a regular feature of the early morning behavior throughout the winter months at Arecibo, and demonstrated that the source of this heating is a flux of fast photoelectrons streaming from the conjugate ionosphere following sunrise in that hemisphere. The onset of the heating has been found to coincide with a solar zenith distance of $\chi = 98°$ to $99°$ when the temperature in the height

range 300 to 400 km is used as an indicator.[23] Heating associated with local sunrise is found to occur at the same zenith distance.

A search has been made for evidence of heating at Millstone Hill coinciding with sunrise at the conjugate point. Unfortunately, the phenomenon cannot be expected in winter at Millstone (Table II) as the conjugate point remains sunlit at that time, and it is not readily possible to distinguish between heat conducted from the protonosphere and a photoelectron flux. Because the conjugate point to Millstone lies south of the Antarctic Circle and about 36 minutes of time further west than Millstone,[4] there is a sunrise at the conjugate point which precedes local sunrise only on about 30 days each equinox. However, an examination of the temperature results obtained during these 30-day periods in 1963 and 1964 does provide evidence for the onset of heating coinciding with conjugate sunrise. Figure 9 shows the electron temperature obtained by averaging values obtained for 300 and 375 km observed on a number of days during these selected periods. The time resolution (~1 hour) in these measurements allows one to distinguish between local and conjugate heating only when the two sunrises are separated by more than about 2 hours. We have attempted to indicate in Fig. 9 the times at which we estimate conjugate and local heating commenced. On April 11, there is only a single abrupt change in $\Delta T_e/\Delta t$ – that associated with local sunrise. On March 15, the temperature begins to rise (at ~2° per minute) approximately 2 hours before local sunrise and continues to do so until local sunrise when there is another abrupt increase ($\Delta T/\Delta t \sim 12°$ per minute). This behavior is similar to that reported by Carlson[20-22] for Arecibo (L ~1.4). At Millstone (L ~3.2), it is possible for conjugate sunrise to precede local sunrise by as much as 4 to 5 hours. In this case, the temperature appears to rise, reach a peak, and then decline to its earlier level (as on 1 March 1963, 3 October 1964). This is distinctly different from the behavior reported[24] by the French group at Nancay (L ~1.8), where, following conjugate sunrise the ionosphere is soon heated to almost its full daytime value, and local sunrise causes no perceptible increase in T_e. The difference in the behavior at Millstone and Nancay must be attributed to the shorter field line length for Nancay with consequent greater transparency to the fast photoelectrons (Sec. IX).

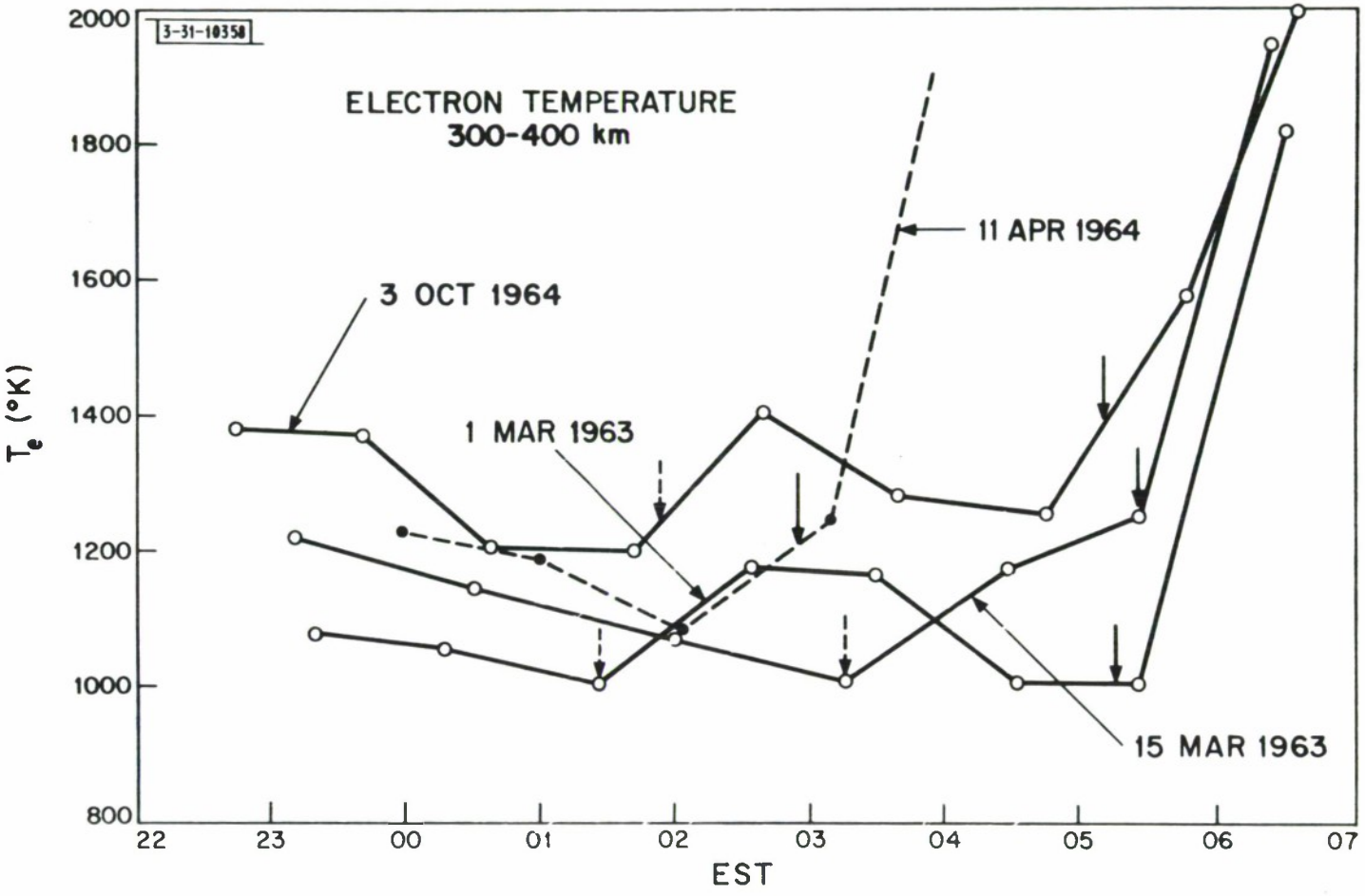

Fig. 9. The variation of T_e showing pre-dawn increases coincident with conjugate sunrise. Solid arrows indicate the time of onset of local heating as estimated from $\Delta T_e/\Delta t$ and broken arrows the time at which conjugate point heating commences.

In order to establish that nocturnal increases of T_e observed during these equinoctial periods are associated with conjugate sunrise, we have plotted in Fig. 10 the times of occurrence together with the time at which $\chi = 98.5°$ at the local and conjugate points. As remarked previously, the poor time resolution afforded by the present measurements does not permit the precise time of the onset of heating to be established, and the bars in Fig. 10 indicate the range of uncertainty. It would appear that both local and conjugate heating commence slightly before a zenith distance $\chi = 98.5°$ is reached, and that the true value probably lies between $\chi = 100°$ and $\chi = 106°$. However, a small shift in the assumed latitude of the conjugate point would make a large change in the value of χ at which conjugate heating would appear to commence.

Theoretical studies of the behavior of the electron temperature during the sunrise have been made by da Rosa[25] who finds that T_e begins to increase as χ reaches 110°. In this analysis, the heat input to the electron gas was assumed to be a Chapman function below 300 km and the Geisler-Bowhill model of midday nonlocal heating[26] (Fig. 11) was assumed above. This seems rather arbitrary as the shadow of the earth's atmosphere must be well above 400 km at $\chi = 110°$ and exact calculations would be required to estimate what effect this must have on the fast photoelectron flux.

VIII. DISCUSSION OF THE RESULTS

A. Daytime Temperature Behavior

The variation of T_e and T_i with altitude may be compared with theoretical predictions by Geisler and Bowhill[13,26] as modified by Banks.[27-29] While the variation of T_i with altitude appears in rough agreement with theory the variation of T_e is in disagreement. In the altitude range 200 to 300 km, the experimental results indicate a slower rise of T_e with height than has been predicted. A re-examination of the theoretical work by Dalgarno and his co-workers (A. Dalgarno private communication) supports this conclusion. In part, the slow rise in T_e with height in this altitude range may be attributed to the poor height resolution achieved in the measurements. However, additional measurements made at oblique incidence with a second radar system[7] do not indicate

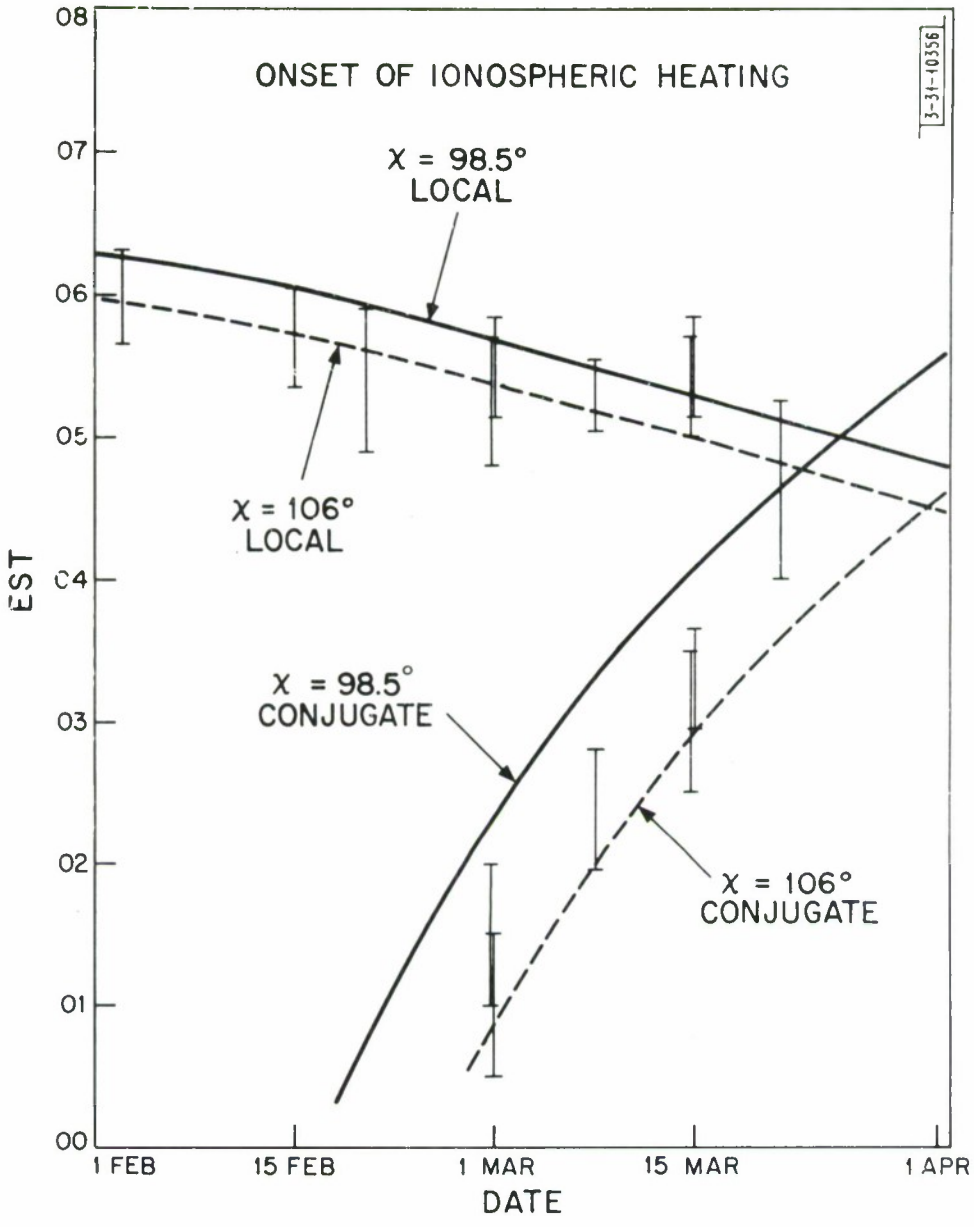

Fig. 10. Times at which local and conjugate sunrise heating appears to commence (Fig. 9). The time at which the sun's zenith distance is 106° and 98.5° is also indicated. These two angles correspond to the earth's shadow reaching 200 km and 100 km, respectively.

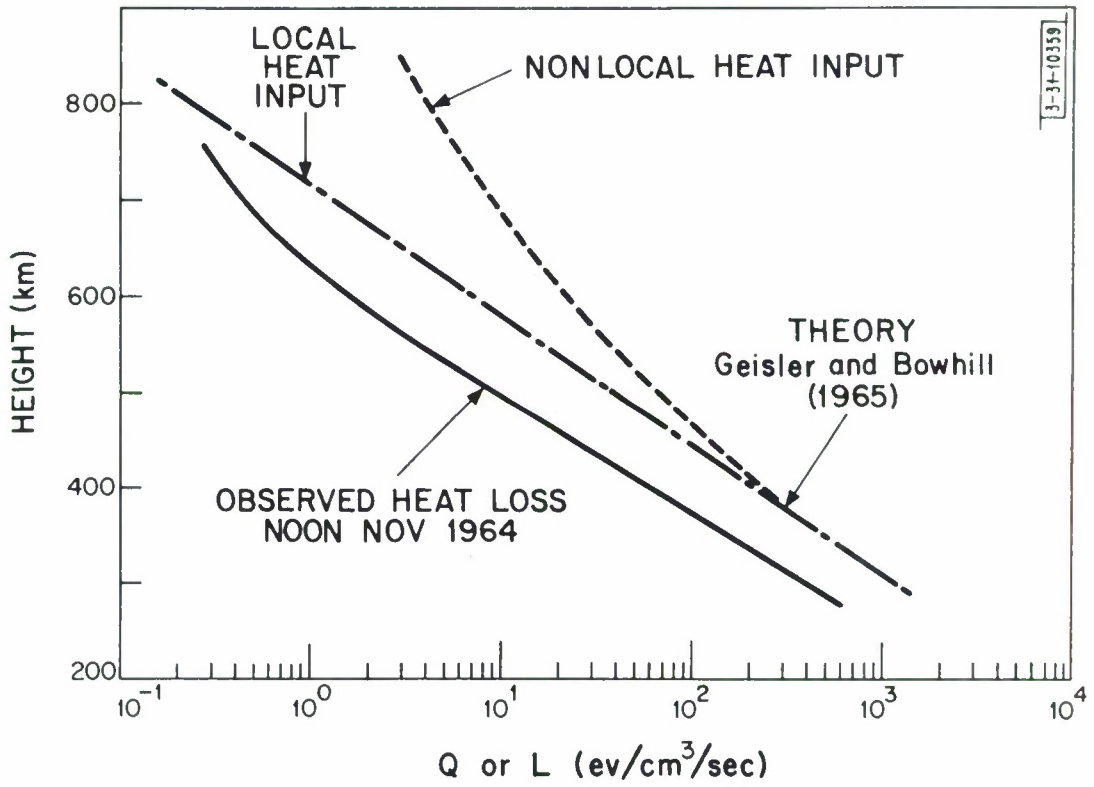

Fig. 11. The heat input to the upper part of the F region according to Geisler and Bowhill.[26] The curve labeled "nonlocal" heating shows the added energy deposited at higher levels by fast photoelectrons escaping from below. The heat-loss curve is the curve computed from Eq. (7) for the density and temperatures observed in November (Fig. 3 a-c) assuming A = 16. This curve represents energy transferred locally to the ions and subsequently conducted via the ion gas to lower altitudes.

substantially better agreement with theory although the height resolution was improved (30 km). Also, some of the results reported by Carru, et al.,[24] appear to exhibit a similar gradual increase over the interval 200 to 300 km although the height resolution was ~10 km. It would seem that only combined rocket and backscatter experiments might be expected to resolve this discrepancy.

A second difference between theory and experiment is that, whereas theory predicts that the region above 300 km should be isothermal,[26,29] the experimental results show a continued rise of T_e with altitude. One might argue that the vertical beam employed at Millstone crosses successive field lines and thus the increase in temperature with geomagnetic latitude observed with

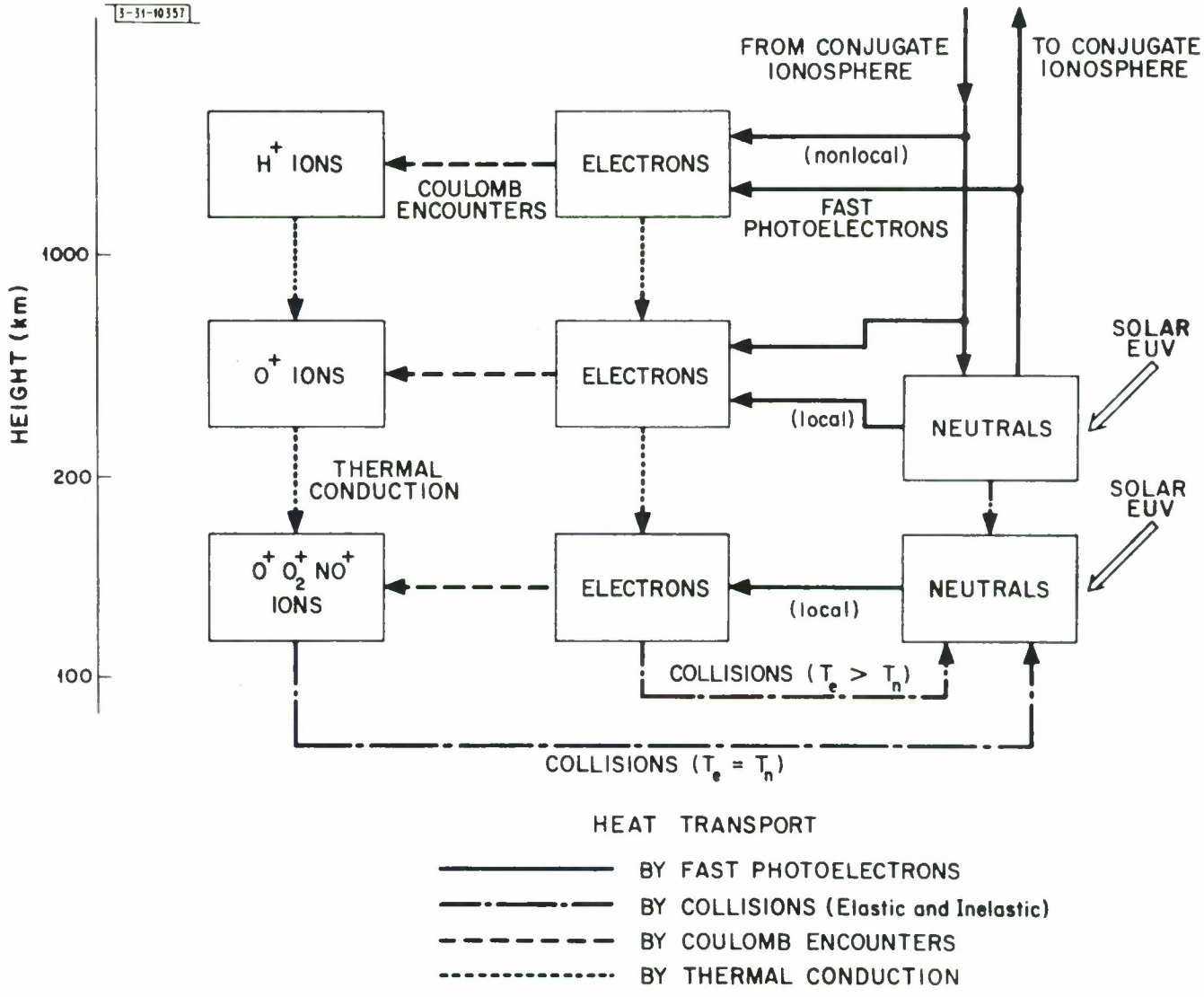

Fig. 12. Block diagram representing in an idealized manner the various heat transfer processes between the electrons, ions, and neutral constituents of the ionosphere.

satellites[30-34] can account for a temperature increase with height. However, if the results of Brace, et al.,[34] are taken as a guide, the temperature increase with latitude is of the order of 0.1°/km, whereas we require an increase of 10°/km to explain the height variation in this way.

Before seeking to explain this phenomenon by modifying current theory, we should first question its reality. We note that such an increase is not indicated by a comparison of the Explorer 17 results at a mean height of 330 km[31,32] for spring 1963 with those of Explorer 22 at 1000 km during spring 1965.[33, 34] However, it may be that conditions changed between 1963 and 1965 so that this is a poor test. The Explorer 17 results when taken alone can be interpreted as indicating an increase in T_e with altitude.[35] Also, Bowen, et al.,[30] found a definite increase in T_e with altitude in this height range using the Ariel I satellite in 1962, which may be real despite the fact that the absolute values reported are systematically lower than those presented here or obtained with other satellites.[2,35] The most convincing argument in support of a temperature increase is that there is agreement between backscatter and satellite results whenever these have been obtained at the same time and place. Thus, the 1963 Explorer 17 results[31,32] agree with backscatter determinations during the same period,[35] and the Explorer 22 results for winter 1964[33,34] agree with values presented here when extrapolated to 1000 km (T_e ~3000°K at midday). Thus, it can be said that there is no obvious reason to doubt the results presented here, although alternative experimental evidence for the temperature rise would be welcome.

The thermal balance for the electrons in the ionosphere has been discussed by a number of authors. Figure 12 gives an idealized diagram of the processes important in the present discussion. Solar ultraviolet radiation gives rise to photoelectron production chiefly at altitudes below 300 km. This process and the subsequent cooling of the fast photoelectrons has been discussed by Hanson,[36] Dalgarno, et al.,[37] and McElroy.[38] Below about 200 km, fast photoelectrons travel only a short distance before being reduced to thermal velocities – principally by inelastic collisions with neutral particles. A small fraction of the excess energy of these photoelectrons is given to the ambient electrons via Coulomb encounters. The electron gas is thereby heated, but loses heat via

collisions with the neutrals and Coulomb encounters with the ions. Above 300 km, a fast photoelectron may travel some distance from the place it is created before it is brought to thermal speeds. Further, since the number of neutrals is decreasing rapidly with height, an increasing fraction of the energy is given to the ambient electrons. Thus, fast photoelectrons traveling upward from the level where they are produced serve to raise the heat input to a value considerably in excess of that deposited by the locally produced photoelectrons at all altitudes above about 500 km. Figure 11 shows the theoretical estimates of the heat deposited by local and nonlocal fast photoelectrons according to Geisler and Bowhill.[26]

A significant fraction of the fast photoelectrons created at altitudes of the order of 300 km and higher have sufficient energy to escape the local ionosphere completely and traverse the protonosphere to the conjugate ionosphere traveling along the lines of force of earth's field. Hanson,[36] who first drew attention to these electrons, estimated their number as 10^9 per second traversing a 1 cm^2 area at 1000 km. More recently, direct experimental evidence for such a flux has been obtained by Carlson,[20-22] Carru, et al.,[24] and ourselves (Sec. VII).

Fast photoelectrons which traverse the protonosphere will deposit some of their energy there, and in this way the temperature of the protonosphere will be raised above that of the F region. The heat will be conducted back down the field line. Geisler and Bowhill[13] estimate that for a latitude of 40° a flux of 10^8 electrons/cm^2 will escape upward from a level near 300 km with an average energy of 10 eV. Upon reaching 1000 km altitude, the average energy will be reduced to 6 eV. A further 3 eV per electron will on average be deposited in the protonosphere.[13] These heating rates lead to only small temperature gradients at all altitudes above 300 km in contrast to the ones reported here. This follows because the thermal conductivity K_e of a fully ionized plasma is very high when the electron temperature is high

$$K_e = 7.7 \times 10^5 \, T_e^{5/2} \text{ eV/cm}^2\text{/sec/°K} \quad . \tag{6}$$

Thus, above 300 km the temperature T_e is largely controlled by the thermal conductivity of the region [Eq. (6)] and the actual heat deposited either locally or by nonlocal photoelectrons is not of great importance.

Thus far, we have omitted the role played by the ions. At all altitudes the ions serve to cool the electrons via Coulomb encounters. Heat is transferred from electrons to ions at a rate

$$L = 7.7 \times 10^{-6} N_e N_i (T_e - T_i) T_e^{-3/2} A^{-1} \text{eV/cm}^3\text{sec} \quad , \tag{7}$$

where N_e and N_i are, respectively, the number density of electrons and ions and A is the mass number of the ion species. Figure 11 shows the heat loss from electrons to ions computed according to Eq. (7) for the mean moon temperature profile for November 1964. It can be seen that the heat transferred from the electrons to the ions is considerably less than that deposited in the region if Geisler and Bowhill's estimates[26] are accepted. The difference represents heat that is conducted down to altitudes lower than 300 km.

At heights below about 300 km, ion-neutral encounters are sufficiently numerous that the neutral and ion temperatures effectively remain the same ($T_i = T_n$). Above about 300 km, this ceases to be true and the ions take up a temperature intermediate between electrons and ions. Hanson[36] and Geisler and Bowhill[26] assumed that eventually (at about 1000 km) $T_i = T_e$. This could be expected because the transition at these altitudes from O^+ to H^+ ions tends to increase the thermal coupling between electrons and ions [Eq. (7)]. Banks,[29] however, has recently shown that the thermal conductivity of the ions cannot be neglected, since it provides a path for heat to lower altitudes (Fig. 12). The ion thermal conductivity is given by[29]

$$K_i = 4.6 \times 10^4 T_i^{5/2} A^{-1/2} \quad . \tag{8}$$

Thus, even though K_i is at least an order of magnitude less than K_e, heat conduction via the ions can serve to maintain a small temperature difference $T_e - T_i$ throughout the protonosphere.[29]

Considering the electron temperature in the region above, say 500 km, we have the following heat conductivity equation which must be satisfied:[26]

$$K_e \sin^2 I \, dT_e = \int_{500}^{\infty} (Q - L) \, dh \quad , \tag{9}$$

where I is the inclination of the field, Q the heat deposited by the fast photoelectrons, and L the loss to the ions [Eq. (7)]. We can make an estimate of $\int_{500}^{\infty} Q \, dh$ by neglecting the losses [Eq. (7)] and then combining Eqs. (6) and (9) to compute $\int_{500}^{\infty} Q \, dh$ from the observed temperature T_e and temperature gradient dT_e/dh at 500 km. Using the mean daytime temperature plot (Fig. 4a), we arrive at the values plotted in Fig. 13a. The values show a summer minimum ($\sim 2.5 \times 10^9$) and a winter maximum of the order of 5×10^9 eV/cm^2/sec. It is possibly significant that the summer minimum occurs in June and hence seems unconnected with the seasonal anomaly (minimum density in August).

The values in Fig. 13a may be compared with Geisler and Bowhill's estimates[26] contained in the nonlocal heat curve of Fig. 11 plus the heat deposited in the protonosphere. In Fig. 11, the scale height of the nonlocal heat curve is $\sim$100 km and the value of Q at 500 km is 70 eV/cm^2/sec, leading to a deposition of 7×10^8 eV/cm^2/sec immediately above 500 km altitude (of which 2×10^8 eV/cm^2/sec is produced by local heating). A further 3×10^8 eV/cm^2/sec is deposited in the protonosphere[13,26] to give a total of 10^9 eV/cm^2/sec available for downward conduction through the 500-km level. The winter day value is observed to be about 5 to 7 times larger (Fig. 13a). This raises the question of whether an additional heat source for the protonosphere exists or if Geisler and Bowhill's estimate is too low.

The rate at which energy is extracted from a beam of fast photoelectrons having a flux ρ energy E and pitch angle with respect to the field α is

$$\frac{dE}{ds} = \frac{-1.95 \, N\rho}{E \cos \alpha} \times 10^{-12} \text{ eV/cm}^2\text{/sec} \quad , \tag{10}$$

where N is the ambient electron density. It follows from Eq. (10) that the transparency of the protonosphere increases with increasing initial photoelectron energy and, consequently, the total energy extracted from the beam is not a sensitive function of the mean initial energy. Thus, in order to deposit more energy in the protonosphere and thereby supply the heat that is observed to be transported downward by conduction, we are required to raise the flux ρ

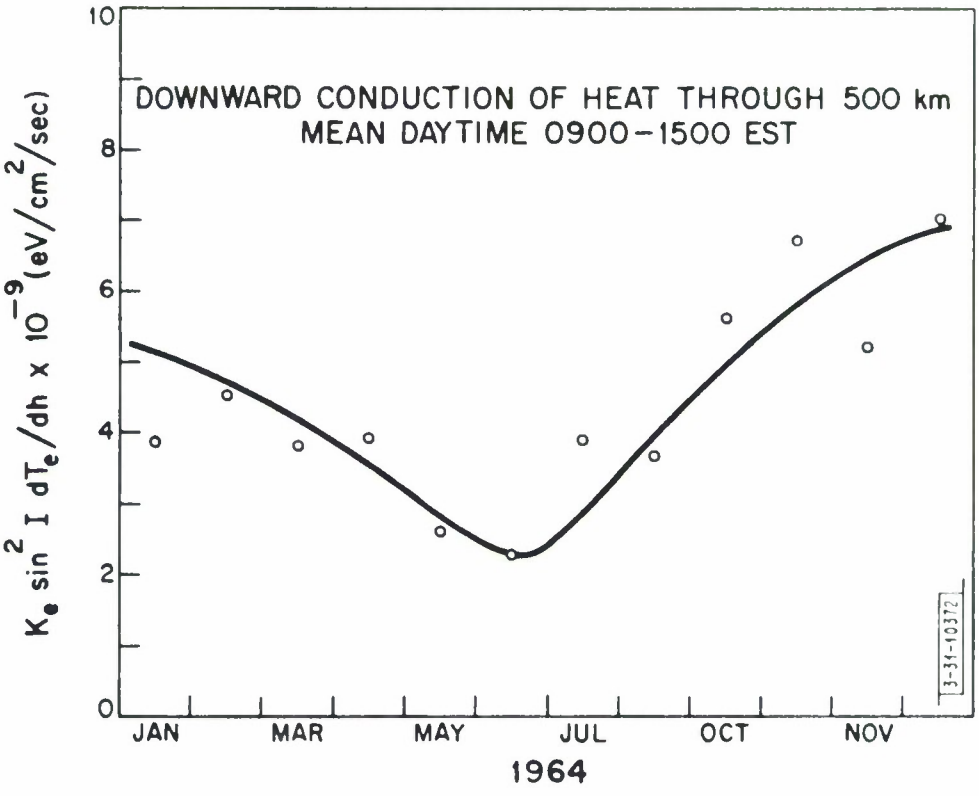

Fig. 13a. The variation of the heat flux from the protonosphere through the 500-km level: (a) corresponding to the mean daytime behavior (Fig. 4a).

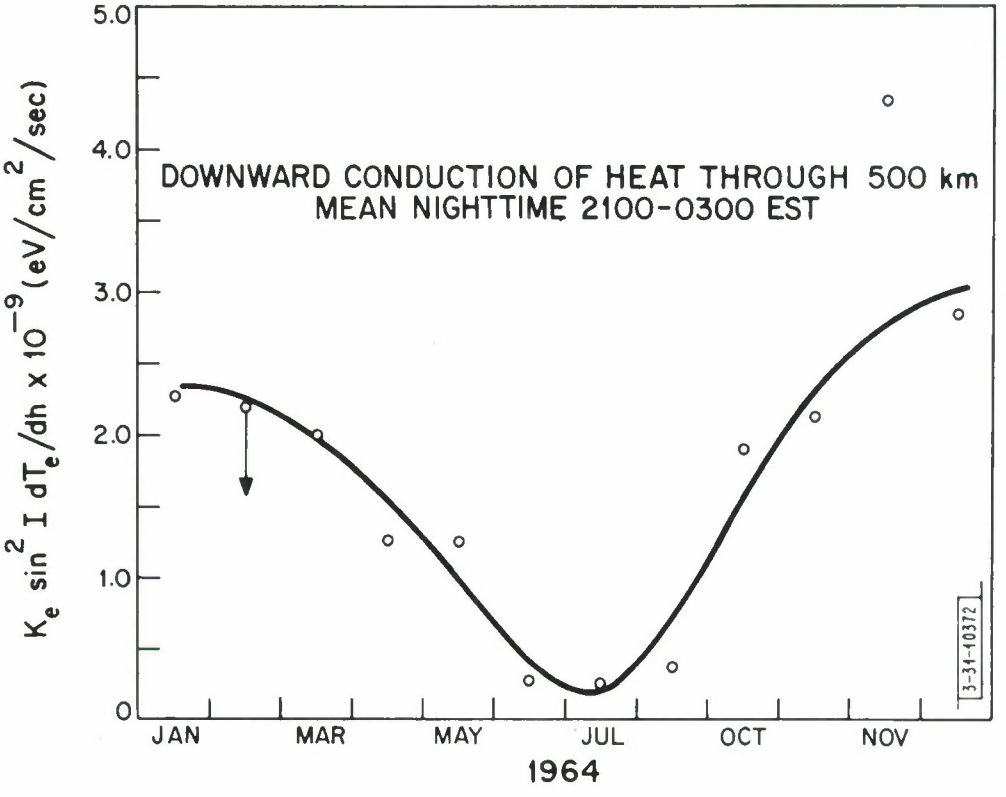

Fig. 13b. The variation of the heat flux from the protonosphere through the 500-km level: (b) corresponding to the mean nighttime behavior (Fig. 4b).

to at least 5 to 7 times that estimated.[13] In other words, no simple modification of the energy spectrum adopted by Geisler and Bowhill[13] can be made to deposit sufficient heat if the flux is maintained only at 10^8 el/cm^2/sec.

B. Nighttime Temperature Behavior

In order to be consistent with the behavior reported in the previous section, we should expect to observe a temperature gradient at night at all altitudes due to the cooling of the protonosphere.[13,14] In winter, when the conjugate point remains sunlit throughout the night (at $\chi = 98°$), we should expect a nighttime heat flux through 500 km about half as large as the daytime flux. This is indeed observed (Fig. 13b). In summer, when both hemispheres experience sunset, the downward supply of heat will be controlled by the rate at which the protonosphere cools, and this in turn is related to the temperature to which the protonosphere was heated prior to sunset and the number of hours that have elapsed since sunset.[14] Thus, in summer, the heat flux is considerably less, and the observed flux of 2.5×10^8 eV/cm^2/sec seems in keeping with the estimates of Gliddon[14] and Geisler and Bowhill.[13]

The variation of electron temperature with time after sunset depends upon the competing influences of the cooling rate [Eq. (7)], which varies as electrons are removed via loss processes, together with the rate at which heat is supplied by the protonosphere. In summer, the temperatures decline throughout the night (Fig. 2b) largely because the heat flux (Fig. 13b) is small and is always decreasing with time.[13,14] In equinox, the temperature begins to increase after ~2200 EST presumably because the density has fallen and N^2 has decreased more rapidly than Q in Eq. (7). This increase follows local sunset ($\chi = 98°$) by about 3 to 4 hours. In winter, the reversal from cooling to heating occurs about 2 to 3 hours after local sunset. The smaller time difference can be attributed to a higher heat flux and lower electron content above h_{max} in winter.

The one anomalous feature that cannot be explained on this basis is the cooling observed in winter between 2200 and 0400 EST (Figs. 3b and c). We have previously[4] sought to explain this as a consequence of the increase in density (Fig. 3a) occurring at this time. This increase was supposed to be a

result of the redistribution of ionization occurring in the tube of force to maintain hydrostatic equilibrium as the tube cools. We supposed that such cooling would be most serious following sunset in the conjugate hemisphere, or in the absence of sunset when the sun's zenith angle becomes large.[4] A closer examination of the altitude of the sun at the conjugate point shows that it is less than $\chi = 90°$ throughout the night and that no change in the angle β between the sun and the field occurs which could cause a significant change in the pitch angle distribution. Thus, although we believe that there is no alternative source than the protonosphere for the increased electron densities observed in the early morning in winter, we no longer have a ready explanation for the redistribution which takes place.

C. The Magnitude of the Conjugate Point Photoelectron Flux

It is difficult to estimate the magnitude of the photoelectron flux from the conjugate point as it does not seem to give rise to a constant heating rate (Sec. VII). That is, the decrease in electron temperature following the initial rise (Fig. 9, 1 March 1963, 3 October 1964) is not understood. There is no increase in electron density at these times which could cause such a phenomenon.

A crude estimate of the flux of fast photoelectrons may be reached from the following argument. Prior to the onset of conjugate point heating the temperature gradient at 500 km indicates the presence of a downward heat flux of $\leqslant 2 \times 10^9$ eV/cm^2/sec (Fig. 13b). The temperature difference $T_e - T_i$ observed at most altitudes is ~600°K and we shall assume that this is directly proportional to the heat flux. After the onset of conjugate point heating, $T_e - T_i$ rises by a further 200°K in the height range 300 to 375 km. Thus, if heat were deposited by the fast particle flux at all levels in the same way as by conduction we would estimate the energy in the particle flux as 7×10^8 eV/cm^2/sec. This is about twice the value (3×10^8 eV/cm^2/sec) estimated by Geisler and Bowhill.[13] In practice, the heat deposited by the fast photoelectrons is restricted roughly to the altitude range of, say, 250 to 650 km, and thus a temperature rise of 200°K in this region is not equivalent to increasing the temperature at all altitudes by this amount. Thus, the above estimate must be too large. On the other hand, the deposition of energy at the foot of the field line which raises the

temperature there will serve to decrease the heat flux conducted from the protonosphere. In view of these uncertain factors, the best that we can do here is place an estimate of 10^9 eV/cm^2/sec on the energy in the fast photoelectron flux. The error in this estimate is probably not larger than a factor of two.

IX. A MODEL FOR THE ESCAPE OF PHOTOELECTRON ENERGY

We have seen that when both hemispheres are sunlit (i.e., in winter) the heat flux traversing 500 km altitude is $\sim 5 - 7 \times 10^9$ eV/cm^2/sec. At night in winter, when only the conjugate ionosphere is sunlit, the heat flux is almost exactly half this amount. The onset of conjugate point heating gives rise to an energy flux in the form of fast photoelectrons of $\sim 10^9$ eV/cm^2/sec, most of which is probably deposited below 500 km.

The photoelectron flux at great altitudes can be examined by observing the enhancement of a feature in the spectrum of the backscattered signals known as the plasma resonance line. Preliminary measurements at the Arecibo Ionospheric Observatory by K. O. Yngvesson indicate a photoelectron density of $0.5^{+0.4}_{-0.2}$ electrons/cm^{3}eV for photoelectrons with energies of 7.5 ± 0.5 eV in the height interval 375 to 500 km.[39] When traveling with zero pitch angle, such electrons would have a velocity of 3×10^8 cm/sec and hence give rise to a flux of 1.5×10^8/cm^2/sec/eV. Allowing for a distribution of pitch angles, Yngvesson estimates a flux of 0.5×10^8/cm^2/sec/eV. In order to integrate over all energies, we refer to the theoretical work of Nagy and Fournier[40] who show that the spectrum of photoelectrons at 300 km is approximately of the form

$$N(E) \cdot dE \propto \exp[-E/7] \quad E \geq 7\,\text{eV} \quad . \tag{11}$$

Assuming that the photoelectrons observed by Yngvesson at 375 to 500 km have this same spectrum, and further that they all escape through the 500-km level, one computes a total escaping energy flux for the range 7 to 30 eV of about 7×10^9 eV/cm^2/sec. This flux comprises 5×10^8 electrons/cm^2/sec with a mean energy of 14 eV per electron.

A fairly self-consistent picture can now be obtained as follows. The energy deposited immediately above 500 km may be taken as five times that

computed by Geisler and Bowhill[13] (due to the increased flux) times a factor 0.7 to allow for the greater transparency due to the higher mean initial energy (14 eV as against 10 eV). This leads to a deposition by nonlocal heating of 1.75×10^9 eV/cm^2/sec which, together with the local heating, leads to an estimate of 1.95×10^9 eV/cm^2/sec deposited immediately above 500 km. Since we require $\sim 10^9$ eV/cm^2/sec to arrive at the conjugate point in the form of fast photoelectrons (Sec. VIII-C), we require the balance (4.25×10^9 eV/cm^2/sec) be deposited in the protonosphere. This requires that the protonosphere be less transparent than computed by Geisler and Bowhill.[13] The heat conducted through the 500-km level will be the sum of the heat input immediately above (i.e., $\sim 1.95 \times 10^9$ eV/cm^2/sec) and that deposited in the protonosphere ($\sim 4.25 \times 10^9$ eV/cm^2/sec), plus that fraction of the energy in the arriving conjugate photoelectrons deposited immediately above 500 km. This yields a total of ≥ 6.2 eV/cm^2/sec as is observed.

Geisler and Bowhill[26] show that if the total electron production is raised by a factor of 5, F region electron temperatures of $\sim 5000°$K should be expected. Presumably, the only way in which to reconcile the flux estimated from the observations with the theoretical estimate is to suppose that the transparency of the neutral atmosphere (which controls the rate of escape at sunspot minimum) is greater than calculated. Possibly the assumption of an isotropic distribution of pitch angles[13] for the photoelectrons also leads to substantial errors.

We are also obliged to ask whether such a large downward heat flux as proposed here can be reconciled with the F region temperatures observed. The heat deposited locally between 200 and 500 km amounts to 3×10^{10} eV/cm^2/sec.[26] Since the downward conducted heat is a factor of five smaller, it seems unlikely that it should lead to a large modification of the temperature observed near h_{max}.

The seasonal variation shown in Figs. 13a and b is open to a qualitative explanation on the following lines. The thermal capacity of the protonosphere will be ~ 3 nk T_{e_t}, where n is the total electron content in the tube of force above 1000 km, k is Boltzmann's constant, and T_{e_t} is the temperature in the

equatorial plane. The day to night change in this capacity will depend upon the day to night variation of T_{e_t} and n. If the variation in n is neglected, we can compute the heat that must be supplied to the protonosphere each day. Taking $n = 4 \times 10^4$ el/cm^2 (Ref. 41), T_{e_t} (day) $- T_{e_t}$ (night) = 1000°K (Ref. 13), we obtain a capacity of $\sim 10^{14}$ eV/cm^2. If heat is injected at a rate of $\sim 10^9$ eV/cm^2 (i.e., both hemispheres sunlit) and heat losses are entirely neglected, it would require $\sim 10^4$ seconds (~3 hours) to raise T_{e_t} to its full daytime value neglecting losses.

It follows that in winter the protonosphere will be close to its full daytime temperature throughout the period 0900 to 1500, since the conjugate hemisphere has been sunlit throughout the night and local sunrise precedes this interval by about 3 hours. In summer, however, conjugate sunrise ($\chi = 98°$) does not begin until a little after 0900 EST, and although local sunrise is earlier the net effect is to lower the midday value of T_{e_t}. A second effect which contributes to a lower value of T_{e_t} in summer is that the distribution of pitch angles of the locally escaping electrons changes between summer and winter.[42] In summer near noon, the sun's rays are directed nearly along the local field line, thereby giving rise to a greater percentage of electrons with pitch angles $\alpha \sim 90°$. Mariani[42] supposes that the reduction in the escaping flux might be as large as a factor of two at this time.

On the basis of the foregoing it seems that the explanation offered in paper 2 for the lower summer electron temperature at high altitudes (namely, the greater thickness of the layer at this time, Fig. 8) is perhaps a related phenomenon but not the prime cause.

X. SUMMARY

A. Daytime Electron Densities

The midday values of $N_{max}F2$ are about twice as large in winter as in midsummer at north temperate latitudes at sunspot minimum. This variation is not reflected in the densities above about 400 km. At these altitudes, the density is a maximum in the equinoxes. As a result, the total electron content observed, for example, by Faraday rotation measurements is a maximum

in the equinoxes, with the summer minimum being deeper than the winter one. The "thickness" of the F region (measured by almost any criterion) is a maximum in summer and minimum in winter.

This pattern of behavior seems unrelated to seasonal variations of the electron, ion or neutral temperatures (this paper, also Ref. 18). We are forced to suppose that the seasonal anomaly is the result of increased loss rates in summer,[43] in agreement with many other workers.[44]

In all seasons, h_{max} is a minimum (~220 km) 2 to 3 hours after ground sunrise and subsequently rises to reach a maximum (~290 km) near midnight. About half of this rise (i.e., one scale height of the ionizable constituent) is accomplished during the daytime.

B. Nighttime Electron Densities

In summer and equinoctial months, the electron density decreases throughout the night. A number of authors have attempted to derive ionospheric loss rates, e.g., from the observed decay of the layer at night[46] or from eclipse results.[47] These have often yielded conflicting results which, in turn, disagree with laboratory values.[48] The latter are usually much higher than values deduced from the behavior of the F region, and this has given rise to a considerable literature on the question of the maintenance of the nighttime F layer.[4,49-52] It appears that at sunspot minimum the cooling of the protonosphere during the night and the subsequent redistribution of the ionization in the tube of force required to maintain hydrostatic equilibrium can supply a flux of electrons large enough to reduce the apparent loss rates by a considerable factor. In winter, the supply of electrons appears to equal or even exceed the loss so that the density either remains constant or increases for a considerable period of the night. It should be noted that the problem of the cooling of a tube of force that was investigated by Geisler and Bowhill[13] has been solved rigorously by Gliddon[14] on the assumption that the electron densities at all altitudes do not change. In actuality, the lowering of the temperature will cause electrons to diffuse to lower altitudes and this, in turn, will serve to convect heat downward. Thus, the problem of the cooling of the protonosphere and the redistribution of the ionization that this produces is a complicated one which still awaits a rigorous solution.

C. Daytime Electron Temperatures

The daytime electron temperatures show a less rapid rise with altitude up to 300 km than has been predicted, and above this altitude a temperature gradient in T_e persists at all altitudes, i.e., in a region that should be isothermal according to theory. It is suggested that theory and observation can largely be reconciled if there is a deposition of heat above 500 km of the order of 6×10^9 eV/cm^2/sec in winter. This might be produced by a flux of photoelectrons through the 500-km level of $\sim 5 \times 10^8$/cm^2/sec (in winter), which deposit 1.75×10^9 eV/cm^2/sec below 1000 km and 4.25 eV/cm^2/sec in the protonosphere.

In summer, the heat conducted down from the protonosphere through 500 km altitude is reduced to about 2.5×10^9 eV/cm^2/sec. It is proposed that the summer to winter difference arises in part because of the absence of any heat input from the conjugate ionosphere for a large part of the day, and in part because the flux of locally escaping photoelectrons is cut down because a large number are created with pitch angles $\alpha \rightarrow 90°$ and fail to escape. The flux of escaping energy estimated here is (in equinox) about 5 times that computed by Geisler and Bowhill,[26] and we suggest that the difference does not arise because the production of electrons is five times higher, but because the factors influencing the escape of photoelectrons (e.g., pitch angle distribution and the transparency of the atmosphere) have been improperly assessed.

Local ionospheric heating appears to commence at a solar zenith distance of $\chi = 102 \pm 3°$. The temperature rise at dawn is especially rapid, and results in an expansion of the F layer which, in turn, lowers the local heat loss rates. The reverse happens at sunset, and causes a rapid redistribution of the electrons above the F layer peak. In summer and equinoctial months, this effect gives rise to a peak in f_oF2 at about ground sunset. The amplitude of the increase in f_oF2 observed in the evening may depend markedly upon the extent to which the layer has risen during the course of the day.

It is concluded that the protonosphere is largely opaque (i.e., a transparency of only ~20 percent) at the latitude of Millstone Hill from the small amount of heating observed locally following conjugate sunrise.

D. Nighttime Electron Temperatures

While there are no major seasonal changes in the mean daytime values of T_e and T_i, the nighttime values exhibit a dramatic variation, being least in summer and greatest in winter. This is attributed to heat supplied from the protonosphere which continues to be warmed by the conjugate ionosphere throughout the winter night and supplies $\sim 2.5 \times 10^9$ eV/cm^2/sec by heat conduction. In summer during the period 2100 to 0300, the heat flux is an order of magnitude smaller and is maintained only by the large reservoir of heat stored in the protonosphere which takes several hours to dissipate. Because the thermal conductivity varies as $T_e^{5/2}$ [Eq. (6)], the heat flux is quite large immediately after sunset, but as T_e falls at the foot of the field line the heat supply is "choked-off" to a much smaller and less rapidly varying value.[13,14]

ACKNOWLEDGMENT

The author would like to acknowledge many members of the staff of the Millstone Hill Radar Observatory for maintaining and operating the ionospheric radar, and in particular, W. A. Reid and J. H. McNally. J. H. MacLeod, J. Upham and Miss D. Tourigny were responsible for the largest part of the data reduction, and Mrs. V. Mason and W. Mason kindly provided the computed signal spectra from which electron and ion temperatures could be obtained by comparison with observed ones. The author is also grateful to the encouragement of P. B. Sebring and V. C. Pineo, and to S. A. Bowhill for many stimulating discussions.

REFERENCES

1. J. V. Evans and M. Loewenthal, Planet Space Sci. 12, 915 (1964).
2. J. V. Evans, Planet Space Sci. 13, 1031 (1965).
3. _____, J. Geophys. Res. 70, 1175 (1965).
4. _____, J. Geophys. Res. 70, 4331 (1965).
5. J. A. Fejer, Can. J. Phys. 38, 1114 (1960).
6. D. R. Moorcroft, J. Geophys. Res. 69, 1436 (1964).
7. J. V. Evans, J. Geophys. Res., in press (1967).
8. S. J. Bauer, J. Atmos. Sci. 19, 276 (1962).
9. S. J. Bauer, Electron Density Profiles in the Ionosphere and Exosphere (ed. J. Frihagen), p. 270, North Holland, Amsterdam (1966).
10. P. J. Bowen, R. L. F. Boyd, W. J. Raitt and A. P. Wilmore, Proc. Roy. Soc. A 281, 504 (1964).
11. T. M. Watt, J. Geophys. Res. 70, 5849 (1965).
12. R. E. Barrington, J. S. Belrose and G. L. Nelms, J. Geophys. Res. 70, 1647 (1965).
13. J. E. Geisler and S. A. Bowhill, J. Atmos. Terr. Phys. 27, 1119 (1965).
14. J. E. C. Gliddon, University of Illinois, Urbana, Aeronomy Lab. Rep. No. 12 (1966).
15. K. C. Yeh and B. J. Flaherty, J. Geophys. Res. 71, 4557 (1966).
16. W. Becker, Electron Density Profiles in the Ionosphere and Exosphere (ed. J. Frihagen), p. 218, North Holland, Amsterdam (1966).
17. L. Thomas, J. Geophys. Res. 71, 1357 (1966).
18. L. G. Jacchia, Space Research V (eds. D. G. King Hele, et al.,), p. 1152 (J. Wiley and Sons, New York, 1966).
19. P. Stubbe, Electron Density Profiles in the Ionosphere and Exosphere (ed. J. Frihagen), p. 249, North Holland, Amsterdam (1966).
20. H. C. Carlson, Electron Density Profiles in the Ionosphere and Exosphere (ed. J. Frihagen), p. 478, North Holland, Amsterdam (1966).
21. _____, J. Geophys. Res. 71, 195 (1966).
22. _____, Cornell University CRSR 212 (1965).
23. _____, paper presented to the International Symposium on Solar Terrestrial Relations, Belgrade (1966).

24. H. Carru, M. Petit and P. Waldteufel, paper presented to the International Symposium on Solar Terrestrial Physics, Belgrade (1966).

25. A. V. da Rosa, J. Geophys. Res. 71, 4107 (1966).

26. J. E. Geisler and S. A. Bowhill, J. Atmos. Terr. Phys. 27, 457 (1965).

27. P. Banks, Institute d'aeronomie Spatiale de Belgique, Aeronomica Acta A No. 45 (1966).

28. _____, Institute d'aeronomie Spatiale de Belgique, Aeronomica Acta A No. 48 (1966).

29. _____, Institute d'aeronomie Spatiale de Belgique, Aeronomica Acta A No. 49 (1966).

30. P. J. Bowen, R. L. F. Boyd, C. L. Henderson and A. P. Wilmore, Proc. Roy. Soc. A281, 526 (1964).

31. L. H. Brace, N. W. Spencer, J. Geophys. Res. 69, 4686 (1964).

32. L. H. Brace, N. W. Spencer and A. Dalgarno, Planet. Space Sci. 13, 647 (1965).

33. L. H. Brace, B. M. Reddy, J. Geophys. Res. 70, 5783 (1965).

34. L. H. Brace, B. M. Reddy, H. G. Mayr, J. Geophys. Res., in press (1966).

35. J. V. Evans, J. Geophys. Res. 70, 4365 (1965).

36. W. B. Hanson, Space Research III (ed. W. Priester) p. 282, North Holland, Amsterdam (1963).

37. A. Dalgarno, B. McElroy and R. J. Moffet, Planet. Space Sci. 11, 463 (1963).

38. B. McElroy, Planet. Space Sci. 13, 403 (1966).

39. W. E. Gordon, paper presented at 15th General Assembly of U.R.S.I. Munich (1966).

40. A. F. Nagy and J. P. Fournier, J. Geophys. Res. 70, 5981 (1966).

41. J. J. Angerami and D. L. Carpenter, J. Geophys. Res. 71, 711 (1966).

42. F. Mariani, J. Geophys. Res. 69, 556 (1964).

43. H. Rishbeth and C.S.G.K. Setty, J. Atmos. Terr. Phys. 20, 263 (1961).

44. G. A. M. King, Planet. Space Sci. 9, 95 (1962).

45. J. W. Wright, J. Geophys. Res. 68, 4379 (1963).

46. J. S. Nisbet and D. McCory in Electron Density Profiles in the Ionosphere and Exosphere (ed. J. Frihagen) p. 530, North Holland, Amsterdam (1965).

47. T. E. Van Zandt, R. B. Norton and G. N. Stonehocker, J. Geophys. Res. 65, 2003 (1960).

48. P. M. G. Dickenson and J. Sayers, Proc. Phys. Soc. 76, 157 (1960).

49. T. Yonezawa, J. of Res. Labs., Japan 12, 65 (1965).

50. _____, Space Research V, p. 49, North Holland, Amsterdam (1965).

51. W. B. Hanson and T. N. L. Patterson, Planet. Space Sci. 11, 1035 (1963).

52. J. E. Geisler and S. A. Bowhill, University of Illinois, Urbana, Aeronomy Lab. Rep. No. 5 (1965).

DOCUMENT CONTROL DATA – R&D

(Security classification of title, body of abstract and indexing annotation must be entered when the overall report is classified)

1. ORIGINATING ACTIVITY *(Corporate author)* Lincoln Laboratory, M. I. T.	2a. REPORT SECURITY CLASSIFICATION Unclassified 2b. GROUP None

3. REPORT TITLE

Midlatitude F Region Densities and Temperatures at Sunspot Minimum

4. DESCRIPTIVE NOTES *(Type of report and inclusive dates)*

Technical Note

5. AUTHOR(S) *(Last name, first name, initial)*

Evans, John V.

6. REPORT DATE	7a. TOTAL NO. OF PAGES	7b. NO. OF REFS
21 August 1967	54	52

8a. CONTRACT OR GRANT NO. AF 19(628)-5167 b. PROJECT NO. 649L c. d.	9a. ORIGINATOR'S REPORT NUMBER(S) Technical Note 1967-41 9b. OTHER REPORT NO(S) *(Any other numbers that may be assigned this report)* ESD-TR-67-479

10. AVAILABILITY/LIMITATION NOTICES

This document has been approved for public release and sale; its distribution is unlimited.

11. SUPPLEMENTARY NOTES	12. SPONSORING MILITARY ACTIVITY
None	Air Force Systems Command, USAF

13. ABSTRACT

Results obtained for F region densities and temperatures using the Millstone Hill Ionospheric Radar for the year 1964 are presented. The measurements were made during 30-hour periods which followed at intervals of about two weeks throughout the year. The data obtained in each month have been averaged to yield a mean electron density profile and mean ion and electron temperature curves for each hour in the day. These curves were in turn used to construct plots showing contours of constant temperature and density as functions of altitude and time for each month. In addition, the annual variation of the midday and midnight densities and temperatures was obtained.

The seasonal anomaly in the F region peak electron density is evident though less pronounced than at years of high sunspot number. The F region layer thickness undergoes a smooth transition from winter to summer, being greatest in summer. It is shown that the daytime temperatures exhibit no marked seasonal dependence, and hence temperature effects (e.g., on reaction rates) cannot be invoked as the cause. The most striking nighttime phenomenon is the high electron temperature encountered in winter ($T_e/T_i \sim 2.0$) compared with summer. Evidence is presented for the existence of a flux of fast photoelectrons arriving from the conjugate ionosphere. The nighttime heating of the F region is thought to be caused by heat conducted down from the protonosphere together, in winter months, with the flux of fast photoelectrons from the conjugate hemisphere. During the daytime, heat appears to be conducted down through the 500-km altitude level at a rate of $\sim 5 \times 10^9$ eV/cm^2/sec. It is not clear whether the heat deposited in the protonosphere by fast photoelectrons is adequate to account for this energy, or if an additional source of daytime protonospheric heating is required.

14. KEY WORDS

F region densities
F region temperatures
sunspot minimum
Millstone Ionospheric Radar